Doctoral Dissertation (Shinshu University)

Human motion detection using an earphone type wearable device and its application to health care

Interdisciplinary Graduate School of Science and Technology,
Shinshu University

Department of Bioscience and Textile Technology

March 2020

KUROSAWA Mami

Abstract

In Japan, interest in personal health care has increased with the graying of society, and the term “healthy life expectancy” has gained prominence year by year. Dietary habits are known to be closely related to lifestyle-related diseases such as obesity, high blood pressure, hyperglycosemia, and hyperlipidemia. Poor chewing and fast eating are especially associated with obesity. Objective evaluation of dietary habits adopted by a nonprofessional person outside of hospital is less effective than the objective evaluation of exercise. Moreover, chewing relates not only to obesity, but also to exercise capacity. People with high chewing potential can self-support their health to a certain degree by maintaining their exercise capacity, and can maintain high nutritional status by eating foods with any degree of hardness. For these reasons, chewing can largely dictate the healthy life expectancy. Therefore, I aim to develop a measurement device that monitors chewing (occlusal force) during mealtimes by an earphone-type wearable device. The device is expected to provide objective evaluations by nonprofessional persons in general environments.

In this thesis, I propose two objective measurement techniques of dietary habits using the earphone-type wearable device. Both evaluation techniques assess the dietary habits at mealtimes to discourage fast eating, and measure the occlusal forces to promote good chewing capacity.

The first technique detects mealtimes among the everyday life activities of the wearer by a small optical sensor inserted into the ear hole of the user. The sensor is composed of a light-emitting diode and a phototransistor, and estimates the mealtimes from the time variations in the amount of received light as the ear canal deforms during chewing. This measurement technique can also measure the body

motions associated with running. Using the data obtained from the ear-inserted optical sensor, the wearer can support a healthy eating, and exercise lifestyle. The proposed algorithm in the wearable ear sensor distinguishes mealtimes and running activities without error, despite the similar characteristics of the two signal types.

The second technique estimates the occlusal force without inserting a sensor into the mouth. The occlusal force during eating can be measured from the movement of the ear canal. Electrode pads, which impede the movement of the masticatory muscle and the jaw joint, are not required. Within the range of occlusal forces exerted by typical healthy adults, this method estimates the occlusal force with comparable accuracy to conventional methods that measure the myoelectricity of the masseter muscle.

The proposed portable mealtime monitoring device and non-intraoral occlusal force meter can contribute to the lifestyle improvement of humans, providing an objective numerical value of the dietary habits in individual homes. Such devices can monitor the exercise quantity and body weight of the user, promoting health self-maintenance by allowing users to review their own state.

Index

Chapter 1: Introduction **1**

1.1 Background 2

1.1.1 Current status of wearable devices 2

1.1.2 Wearable device on health care 4

1.1.3 Earphone type wearable device 5

1.1.4 Significance of the human motion detection using an earphone type wearable device 6

1.2 Targets for measurement 7

1.2.1 Meal time 8

1.2.2 Occlusal force 8

1.2.3 Utilization of the earphone type wearable sensor to health care 9

1.3 Organization of this thesis 9

Chapter 2: Mealtime detection using an earphone type sensor 13

2.1 Background and objectives 14

2.2 Materials and methods 16

2.2.1 Measurement principle and sensor prototype 16

2.2.2 Meal time estimation algorithm 20

2.2.3 Data collection protocol 25

2.3 Results 27

2.4 Discussion 32

2.5 Conclusion 36

Chapter 3: A basic study for estimation of occlusal force using an earphone type sensor 37

3.1 Introduction 38

3.2 Methods 40

3.2.1 Overview of experiments 40

3.2.2 Experimental system 40

3.2.3 Subjects 43

3.2.4 Experimental methods 43

3.2.4.1 Measurement of characteristics of occlusal force sensor 43

3.2.4.2 Correlation between outputs of occlusal force sensor and ear sensor 44

3.2.4.3 Estimation of occlusal force from ear canal movement 44
3.3 Results 46
3.3.1 Results of measurement of occlusal force sensor characteristics 46
3.3.2 Results for correlation between outputs of occlusal force sensor and ear sensor 46
3.3.3 Results for estimation of occlusal force from ear canal movement 50
3.4 Discussion 52
3.5 Conclusion 54

Chapter 4: Simultaneous Measurement of Ear Canal Movement, Electromyography of the Masseter Muscle and Occlusal Force 56
4.1 Introduction 57
4.2 Materials and Methods 59
4.2.1 Experimental System 59
4.2.2 Subjects 64
4.2.3 Simultaneous Measurement of Ear Canal Movement, Masseter Muscle Electric Potential and Occlusal Force 65
4.2.4 Method of Occlusal Force Estimation from Ear Canal Movement Measured by Ear Sensor and Associated Evaluation Method 66
4.3 Results 68
4.3.1 Simultaneous Measurement Results for Ear Canal Movement, Masseter Muscleand Occlusal Force for Earphone-Type Occlusal Force Sensor 68
4.3.2 Results for Estimation of Occlusal Force from Ear Canal Movement (Ear Sensor Value) 72
4.4 Discussion 75
4.5 Conclusion 79

Chapter 5: Conclusions 82

Chapter 6: References 86

Chapter 7: Accomplishments 93
7.1 Publications in Journal 94
6.2 Conferences 94

Chapter 8: Acknowledgement 97

Chapter 1:

Introduction

1.1 Background

1.1.1 Current status of wearable devices

Wearable devices are used in various scenarios such as daily life support, sports coaching, healthcare monitoring, and vital-signs management [1]. Most wearable devices are shaped as accessories such as watches and wristbands, which directly contact the skin of the wearer. These products consist of plural sensors arranged to suit their purpose, as shown in Figure 1.1.

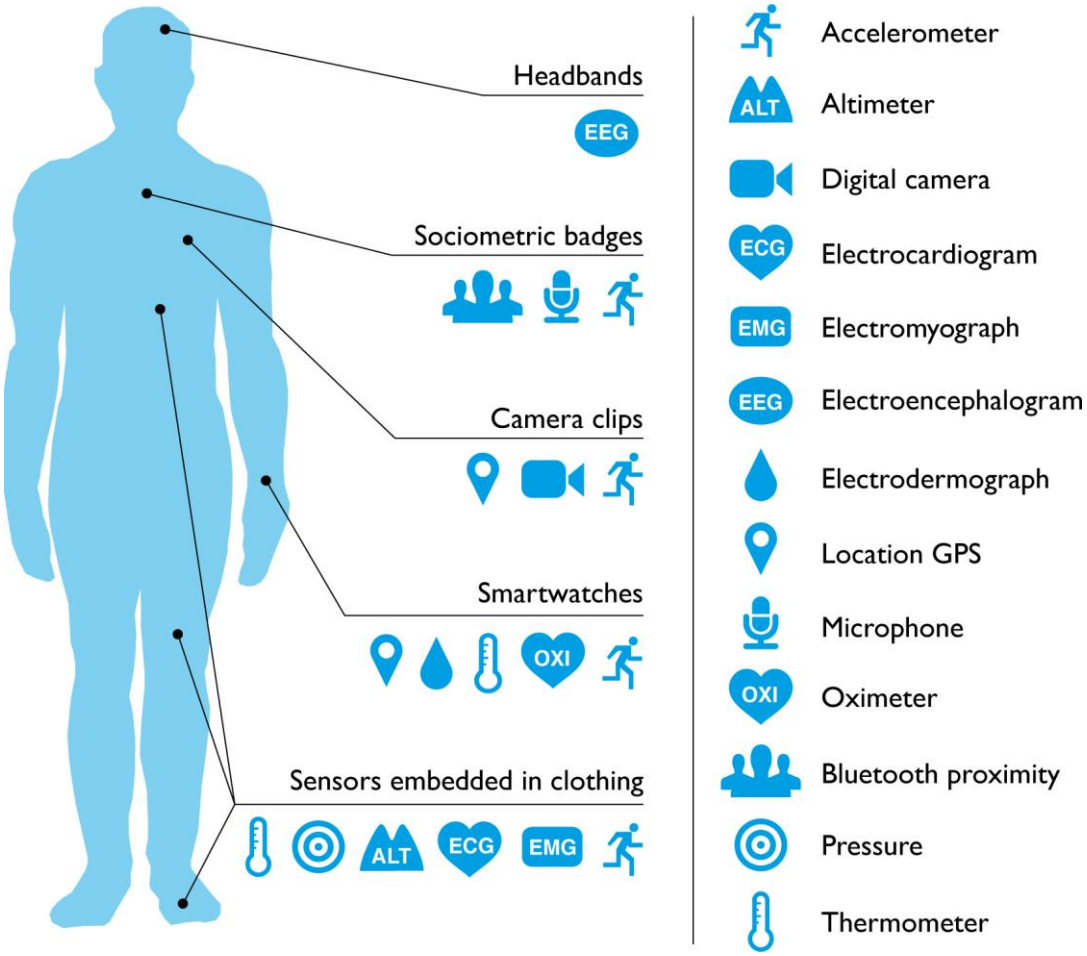

Figure1. 1. Various scenarios of consumer wearables [2]

A wearable device measures various biological information. The recorded and visualized activity data are used to improve the operational efficiency and self-

management of the wearer. The information is processed by a portable computer such as a smart phone or tablet terminal. Irrespective of other movements, a wearable device such as a smart watch continuously collects information and communications throughout the day without the user's awareness, unless the user's movements are obstructed. In contrast, a smartphone is carried and used consciously.

The future development of wearable devices is expected to be divided into four main categories: smart textiles, systems and applications, situation recognition, and human–computer interactions [3]. The technological developments and the themes attracting attention in each category are outlined below.

(1) Smart textiles

Design, usage, and evaluation remains an important field in wearable computer study. The development of mature electronic systems such as electronic matrix fibers with elasticity is gaining traction.

(2) Systems and applications

Research hotspots are the utilization of wearable devices in health and exercise, and their cooperation with other wearable systems as new wearable applications.

(3) Situation recognition

Situation recognition by sensors attached to the body have long been the mainstay of wearable computer study. Current topics are the feasibility of dynamic sensor configurations previously learned from recognition systems in complicated and difficult situations.

(4) Human–computer interactions

Wearable computer study is dominated by interactions between humans and portable devices. Important issues are communication with a portable

device and the improved flexibility of other interfaces such as textile products.

1.1.2 Wearable devices in health care

With each passing year, interest in personal healthcare has increased with the graying of Japanese society and the growing emphasis on “healthy life expectancy.”

Smart watches can record the wearer’s walking distance and heart rate in real-time. Besides warning the user of sudden rises in heart rate, a smart watch makes an emergency call with a preset application when it detects a cardiopulmonary arrest.

Wear utilizing hitoe hitoe transmitter Smartphone

Figure1. 2. Technology of “hitoe” [4]

The hitoe device [4] (Nippon Telegraph and Telephone Corporation, Toray industries Inc.) is a wearable device for health-risk management. Hitoe detects heat stroke during exercise and assesses the health condition of long-distance drivers and workers at construction sites, thus preventing diseases and accidents. The hitoe device is sewn inside a sports T-shirt and directly touches the skin above the heart. A data transmitter that downlinks to a recording medium is worn outside the sportswear,

as shown in Figure 1.2. During training, this transmitter sends the heartbeat information into a recording medium and a computing apparatus in a smartphone.

1.1.3 Earphone-type wearable device

The body of earable is a standard earphone for music players. The body contains an optical distance sensor that measures distance changes of the ear canal. The light emitted from the diode inside the earphone is reflected back by the eardrum and the ear canal. The amount of light received at the sensor depends on the distance between the sensor and the eardrum and between the sensor and the ear canal (Figure 1.4). During chewing, the ear canal moves in conjunction with the masticatory muscle operating the jaw, because the two structures are contiguous. Other facial or head motions such as eye blinking, nodding, and tongue motions also influence the state of the ear canal. By analyzing the amount of receiving light and the characteristics of the transition, the device can detect jaw and body movements [5, 6], tongue movements [7], breathing rates [8], and concentration states from the breathing rate and head-shaking movements [9].

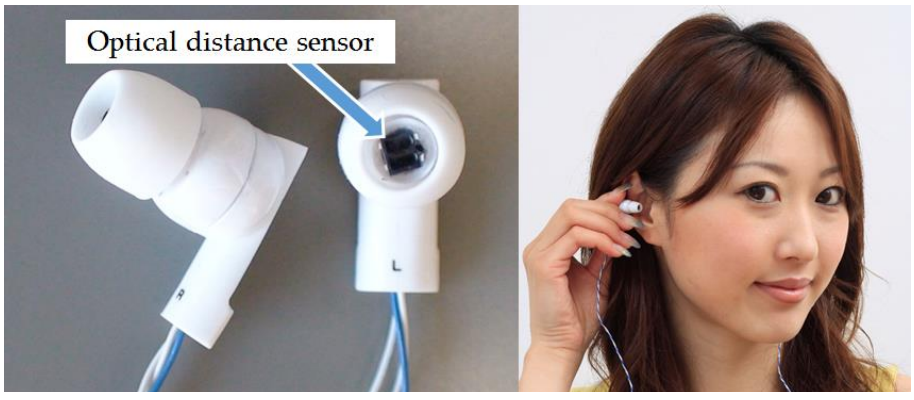

Figure1. 3. Appearance of “earable”

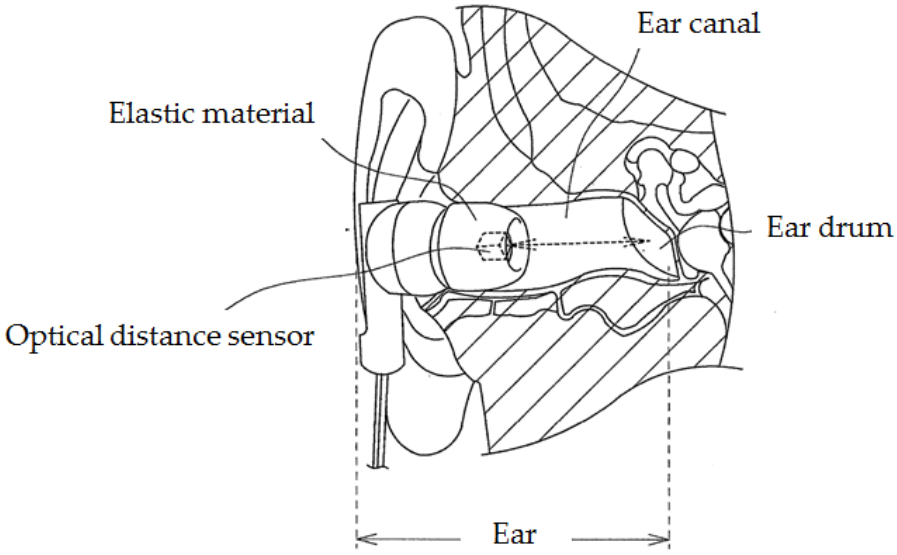

Figure 1. 4. Measurement principle of earable [5]

1.1.4 Significance of human motion detection using an earphone-type wearable device

The earphone-type wearable device is more easily integrated into everyday life and can be worn for a longer time than other wearable devices, because it does not disturb the wearer's hand and eye movements. Meanwhile, the hearing sense is unaffected unless the device completely blocks the earhole. Furthermore, earable can gather the face information, which is difficult to measure by wearable devices placed on the limbs. The device is easily arranged on the body (like other wearable devices), and is merely inserted into the ear like a regular earphone.

The earphone-type wearable device provides an objective evaluation for nonprofessional persons in general environments. It assists health self-maintenance by reviewing the wearer's own state and outputting an objective numerical value reflecting the wearer's dietary habits in his or her home, similarly to an exercise monitoring meter and a body weight meter.

1.2 Targets for measurement

Based on the characteristics in Section 1.1.4, I develop a “how to eat” measure of health, alongside exercise monitoring. As is well-known, poor dietary habit is closely related to lifestyle-related diseases such as obesity, high blood pressure, hyperglycosemia, and hyperlipidemia. Poor chewing and fast eating are especially associated with obesity [10, 11]. In dietary counseling, a medical staff member guides the slowing down eating and promotes good chewing. However, an objective measure of chewing amount in a self-made effort, such as counting the chews, is lacking.

Chewing is related not only to obesity, but also to exercise capacity [12]. People with high chewing potential can largely self-support a high exercise capacity, and can maintain good nutritional status because their meal choices are not limited to soft food materials. Thus, chewing deeply relates to the extent of a healthy life expectancy.

One objective indicator of chewing is the value measured by an occlusal force meter. However, this value is not a suitable health care index in the present case, because the continuously measured data of the same person by an occlusal force meter must be corrected by a medical specialist [13].

Two elements in a person’s dietary habit are important for extending the healthy life expectancy. First, meals should be eaten leisurely at regular and appropriate times. Second, the bite force (occlusal force) should be sufficient for consuming various foods without hesitating.

The aim of this thesis is to develop techniques for measuring these two elements, and hence support health maintenance by an objective evaluation.

1.2.1 Mealtimes

In dietary support, the measured results of meals are as important as the measured results of exercise amount. Calorie control is the main form of mealtime support, but support based on mealtime management is growing in popularity. Irregular meal times and eating before bedtime are among the factors that promote the onset and progression of lifestyle-related diseases [14]. However, mealtime management support for ordinary individuals remains limited by various challenges, namely, lack of awareness on the importance of mealtimes in society, and the lack of wearable devices that can easily, and automatically estimate mealtimes without interfering with lifestyle.

1.2.2 Occlusal force

The elderly population is growing steadily, spurring the demand for technologies that monitor dental occlusion and chewing. Improving the meal-intake method of elderly people is important for preventing nutritional disorders. Good chewing ability is reported to greatly extend their healthy life expectancy [13, 15]; moreover, epidemiological studies report that chewing ability in the elderly is closely related not only to bodily functioning, but also to mental activities, and even vital functions [16].

Patients who undergo a gastrectomy operation for gastric cancer are at increased risk of nutritional disorders because their gastric function is reduced [17]. The meal-intake method of such patients would be improved by ensuring that their food is well chewed; that is, by ensuring sufficient occlusal force.

1.2.3 Utilization of the earphone-type wearable sensor in health care

A reliable earphone-type chewing-count measurement device has been researched and developed by a co-researcher of the present study [18]. To measure the number of chews performed by the user, this device detects the ear canal movements by the earphone-type sensor (ear sensor) embedded within it. The device displays the total number of chews on a tablet terminal in real-time. It also records the number of chews and the measured waveform on the tablet. The device is used in experimental analyses of the dietary behaviors of adipose patients, and in the provision of meal instructions for post-gastrectomy patients in a medical institution in Japan.

Based on the present research, we considered that the signals of the ear sensor reflect the volumes of movement and power. I thus aim to develop two techniques using the ear sensor, which closely relate to dietary healthcare. First is the detection of mealtimes among daily life activities, and second is the measurement of occlusal force by the device, which then acts as a non-intraoral type occlusal force sensor.

1.3 Organization of this thesis

The remainder of this thesis is organized as follows.

In Chapter 2, I describe the technique for estimating meal times by the earphone-type wearable sensor. A small optical sensor composed of a light-emitting diode and phototransistor is inserted into the ear hole of the user. The device estimates the mealtimes of the user from the time variations in the amount of light received. To this end, the light is emitted toward the inside of the ear canal and is reflected back

from the canal wall. The proposed technique differentiates meals from other activities such as conversing, sneezing, walking, ascending, and descending stairs, operating a computer, and using a smartphone. When food intake is measured by conventional devices worn on the heads of users, the measurements are affected by movements such as running, which introduce strong vibrations as the body is jolted more violently than during walking. In such cases, conventional devices can misclassify running as eating. The data transitions during running and chewing share similar characteristics. Preventing confusion with other movements is important for daily life monitoring, and bars the use of conventional sensors as monitoring devices. To solve this problem, I simultaneously insert a wearable ear sensor into the left ear and another sensor in the right ear. The measurements from the left and right ear canals are strongly correlated during running, but are uncorrelated during eating. This difference is caused by the uneven chewing of food on the teeth of both sides. Therefore, running and eating can be distinguished from their correlation coefficients, thus reducing the misidentification instances. Moreover, the semiconductor-based optical sensor realizes a small and lightweight device. Because the same measurement technique can measure the body motions associated with running and eating, the data obtained from the optical sensor can support a healthy lifestyle regarding both eating and exercise.

In Chapter 3, I investigate the correlation between occlusal force and the movement of the ear canal. Through this basic study, I investigated my aim of measuring the occlusal force by the earphone-type wearable device. For health maintenance by chewing and eating, the amount and time of chewing dictate the digestibility of the food, and the biting power should be sufficient for consuming various foods. Supporting occlusal force maintenance is expected to extend the healthy life expectancy. Therefore, dentists require an objective and continuous

device that measures the occlusal force of a given patient. I here propose a measurement technique for occlusal force using the wearable ear sensor, which is easily used by non-professionals in daily life. The proposed estimation method uses the least-squares method and the weighted average. The experimental device, which simultaneously measures the occlusal force and the ear canal movements, primarily consists of an occlusal force sensor, and a wearable ear sensor. The analog signals from both sensors are converted into digital signals by an analog-to-digital converter. The data are then recorded as signals associated with the measurement time. Six experimental subjects were requested to chew for two seconds while their masticating force was measured by the occlusal force sensor. The experiment was performed five times. The occlusal force sensor was placed on the right second molar, and the wearable ear sensor was placed in the right ear. Throughout the experiment, the occlusion, and the ear canal movements were strongly correlated. The average correlation coefficients consistently exceeded 0.89 for all subjects.

In Chapter 4, I proposed a measurement technique of occlusal force by the wearable ear sensor. To this end, I simultaneously measured the ear canal movements (ear sensor values), the surface electromyography (EMG) of the masseter muscle, and the occlusal force of five subjects following the study of Chapter 3. This experiment was performed six times per subject. I then investigated the correlation coefficient between the ear sensor value and the occlusal force, and the partial correlation coefficient between the ear sensor values. Additionally, I averaged the partial correlation coefficients and considered the absolute value of the average for each subject. The absolute values of the coefficient were strongly correlated for all subjects. Partial correlations between the ear sensor values and the occlusal forces were also confirmed in each subject. Finally, I estimated the occlusal force exerted by each subject in a regression analysis, and evaluated the proposed method by the

cross-validation method. The root-mean-squared error between the actual and estimated values was evaluated for each of the five subjects.

Chapters 5, 6, and 7 give the overall conclusions, accomplishments, and acknowledgments of the thesis, respectively.

Chapter 2:
Mealtime detection
using an earphone type sensor

2.1 Background and objectives

The use of wearable devices is growing in popularity in the field of healthcare [19–34]. Wristwatch-type wearable devices are particularly widespread and estimate the amount of exercise by measuring body temperature and heart rate, thereby supporting a users' diet by presenting these estimates to users. In dietary support, the use of measured results for meals is just as important as support that uses measured results for the amount of exercise. Calorie control is the main form of support for meals; however, support using meal time management has recently received growing attention. Irregular meal times and eating before bedtime have been found to be some of the factors that promote the onset and progression of lifestyle-related diseases [14]. However, support for ordinary individuals using meal time management remains limited due to some challenges, including the lack of awareness among society regarding the importance of meal times and the lack of wearable devices that can easily and automatically estimate meal times without interfering with lifestyle.

Recently, measurements of food intake have been performed using eyeglass-type wearable devices [37]. Eyeglass-type devices use optical, strain, and other sensors to measure food intake. Strain sensors require close contact between the sensor and skin during measurement, whereas optical sensors can take measurements without bringing the sensor in close contact with the skin. Thus, optical sensors have a greater advantage over strain sensors as they are minimally impacted by the shape and amount hair growth on the surface of a user's skin. Moreover, studies that have used strain sensors have been able to differentiate walking from eating by combining strain sensors with accelerometers. In eyeglass-type devices, the vibration of the devices themselves during walking affects the measured data; however, these

measured values obtained from walking can be removed because they are smaller than the values measured during chewing. However, violent body motion (e.g., during running) also increases the vibration of the device itself, which can increase the effect on the values measured by this vibration, making it difficult to remove. A device can be fixed to a user's head to minimize vibrations; however, this is more uncomfortable for a user. Therefore, vibrations of a device due to running are a difficult issue to overcome with eyeglass-type wearable devices.

The objective of my study was to develop a wearable device capable of measuring food intake and differentiating eating from running. In this chapter, we described a technique for estimating meal times as the first stage in reporting these research results. The measurements of food intake by eyeglass-type devices use a sensor to measure the "movement of the masticatory muscles, including mainly the temporal muscle (temporalis)" and "movement of the skin in the temporal region resulting from the movement of the temporomandibular joint (TMJ)." I discussed the measurements of chewing from the relationship between the anatomical position of the temporal muscle and TMJ in humans, as shown in Figure 2.1, and revealed that changes to the shape of the ear canal during chewing are useful for measuring food intake [5]. While the shape of the ear canal also changes during facial expressions [6], chewing tends to repeatedly change the ear canal shape, which makes it possible to distinguish chewing from facial expressions. In this chapter, I described a technique for estimating the meal times of users based on temporal changes in the amount of light received by a small optical sensor composed of a light-emitting diode (LED) and phototransistor inserted into the ear hole, which emits light toward the inside of the ear canal and receives light reflected back from the ear canal, to measure the change in the amount of light. I also proposed a method for differentiating eating from running.

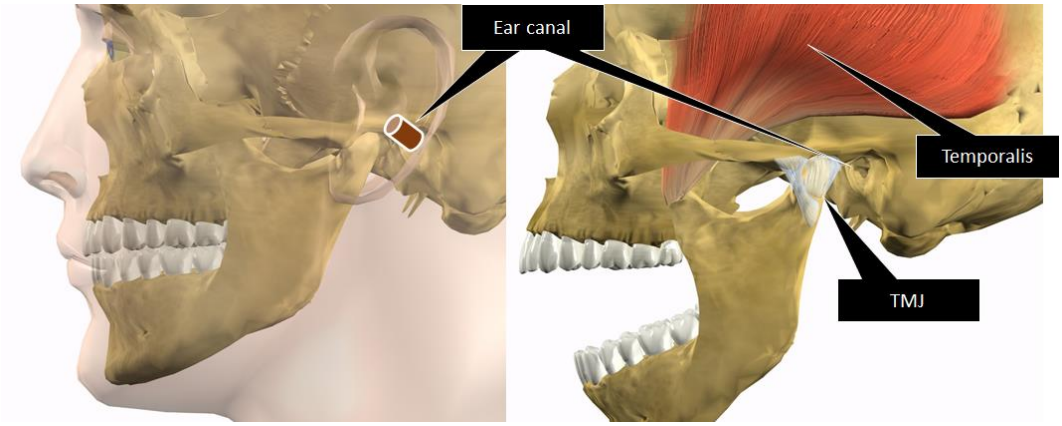

Figure 2.1. Anatomical positional relationship between the ear canal, temporal muscle (temporalis), and TMJ. Chewing occurs by moving the TMJ and the temporal muscle. The ear canal is anatomically close to the TMJ and temporal muscle and is susceptible to mechanical force exerted by the TMJ and temporal muscle.

2.2 Materials and methods

2.2.1 Measurement principle and sensor prototype

Figure 2.2 presents a schematic diagram of a sensor designed to estimate meal times. The sensor in Figure 2.2 measures movement in the ear associated with eating. Using this method, movement in the ear is measured by light. Using light, eating can be measured without the sensor irritating the sensitive ear. Eating measurements are done by inserting an earphone-type sensor into the ear hole (ear canal), as shown in Figure 2.2. This earphone-type sensor has a built-in optical distance sensor that is composed of a light-emitting portion (LED) and a light-receiving portion (phototransistor). The earphone-type sensor receives the light emitted from the optical distance sensor that is reflected back by the eardrum and ear canal. During chewing, the shape of the ear canal changes, which alters the distance between the optical distance sensor and the eardrum and ear canal. The amount of

light received changes over time in association with this change in distance. In this study, I estimated meal times by analyzing temporal changes in the amount of light. The LED of the optical distance sensor used in the earphone-type sensor emits infrared light at a wavelength of 940 nm, which is rare in the natural world (sunlight does not contain a substantial amount of this wavelength of infrared light).

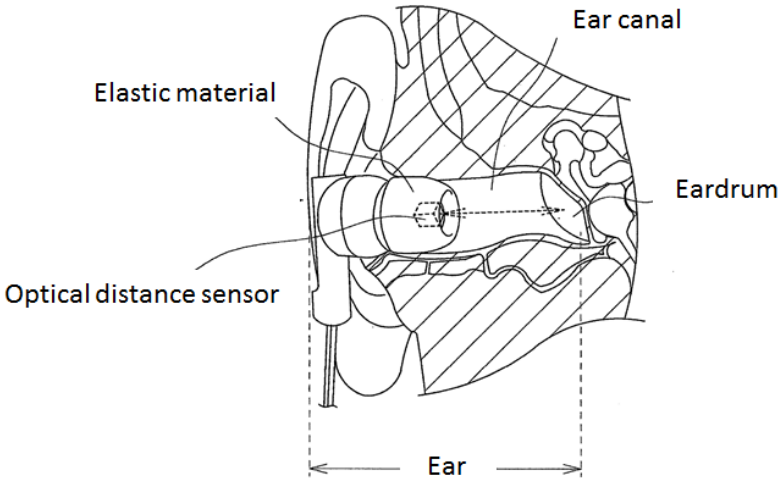

Figure 2.2. Measurement principle for changes in the shape of the ear canal. The earphone-type sensor receives the light emitted from the optical distance sensor that is reflected back by the eardrum and ear canal. During chewing, the shape of the ear canal changes, which alters the distance between the optical distance sensor and the eardrum and ear canal. The amount of light received changes over time in association with this change in distance.

The optical distance sensor within the earphone-type sensor takes measurements within the closed space of the ear canal, which limits the effect of light from outside the body and does not restrict the environments in which a user can employ the sensor (it can be used both indoors and outdoors, during summer and winter, and in the day and at night). While the earphone-type sensor only vibrates slightly as a result of intense movement (e.g., running), the sensor is securely surrounded by the ear canal, which minimizes vibrations compared with eyeglass-type devices. The earphone-type sensor is also fitted with an optical distance sensor

inside a casing that is the same as that widely used in conventional inner ear-type earphones, which allows the earphone-type sensor to be worn as easily as a conventional earphone.

Figure 2.3 shows the outer appearance of the prototype earphone-type sensor, while Figure 2.4 is a representation of its electronic circuit. As shown in Figure 2.3, the earphone-type sensor has the same shape as a conventional inner ear-type earphone, and is worn and used in both ears. This prototype optical distance sensor uses a KODENSHI SG-105 photo reflector (a Fairchild QRE1113 Reflective Object Sensor can also be used). As shown in Figure 2.3, infrared light from an LED is in the vicinity of the eardrum and is received by a phototransistor by placing an optical distance sensor in the same casing as a conventional inner ear-type earphone. In the circuit presented in Figure 2.4, it is evident that the reflected light changes based on the distance d between the phototransistor and vicinity of the eardrum, which causes the collector current IC of the phototransistor to change in response to fluctuations in the shape of the ear canal associated with chewing. The change in the collector current IC obtained here is converted into a change in the voltage of the resistor RL. This change in voltage is considered as the output voltage of the sensor.

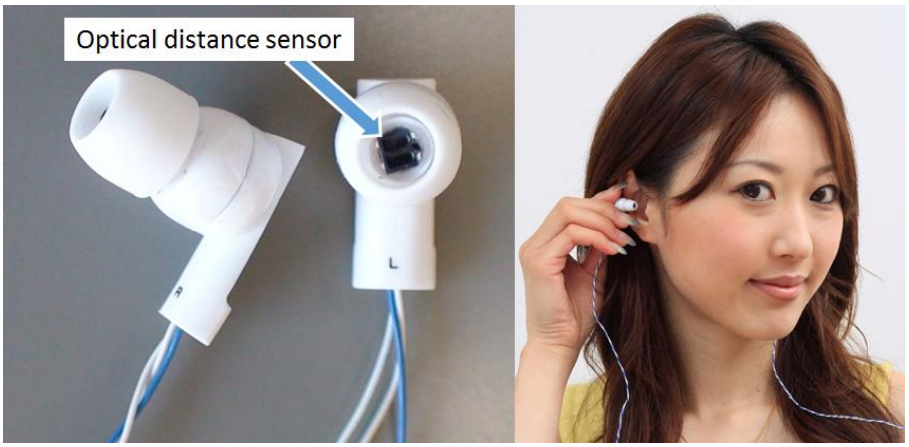

Figure 2.3. Sensor prototype. The earphone-type sensor has the same shape as a conventional inner ear-type earphone. The sensor is worn and used in both ears.

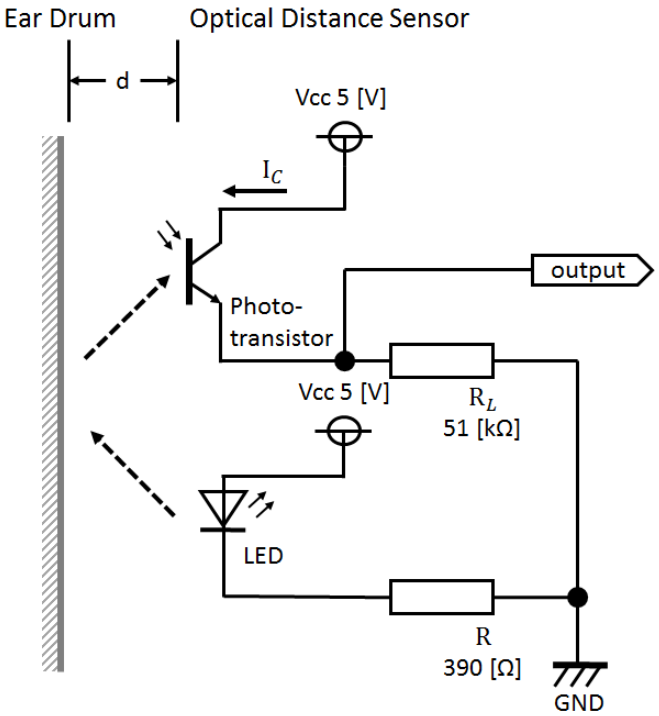

Figure 2.4. Electronic circuit around the sensor. The circuit is evident that the reflected light changes based on the distance d between the phototransistor and vicinity of the eardrum, which causes the collector current I_C of the phototransistor to change in response to fluctuations in the shape of the ear canal associated with chewing. The change in the collector current I_C obtained here is converted into a change in the voltage of the resistor R_L. This change in voltage is considered as the output voltage of the sensor.

2.2.2 Meal time estimation algorithm

To obtain preliminary data to design a meal time estimation algorithm, I measured the movement of the ear canal of subject X by means of the earphone-type sensor shown in Figure 2.4. The measured results are presented in Figures 2.5–2.7. Figure 2.5 (a) shows the measured values for movement of the ear canal during conversations, and Figure 2.5 (b) presents the amount of change in these measured values. The amount of change was obtained by subtracting the immediately anteceding measured value (100 ms prior to obtaining measurements because measurements are performed at 10 Hz) from the current measured value. Figure 2.6 (a) shows the movement of the ear canal during yawning, while Figure 2.6 (b) shows the corresponding amount of change. Figure 2.7 (a) presents the movement of the ear canal while chewing gum, while Figure 2.7 (b) shows the corresponding amount of change. Figures 2.5 (b) and 2.7 (b) show that the amount of change is 3.42×10^{-2} V during conversations and 1.42×10^{-1} V while chewing gum. A comparison of the amount of change during conversations and chewing gum reveals that the amount of change is greater during chewing gum; this is because the movement of the ear canal is greater. Furthermore, Figure 2.6 shows that the amount of change during yawning is 1.17×10^{-1} V, which is similar to the amount of change during chewing and greater than the amount of change during conversations. Yawning and chewing gum are similar in that they involve greater movement of the ear canal than conversation. However, a comparison of Figures 2.6 and 2.7 reveals that chewing gum is characterized by a large “continuous” change.

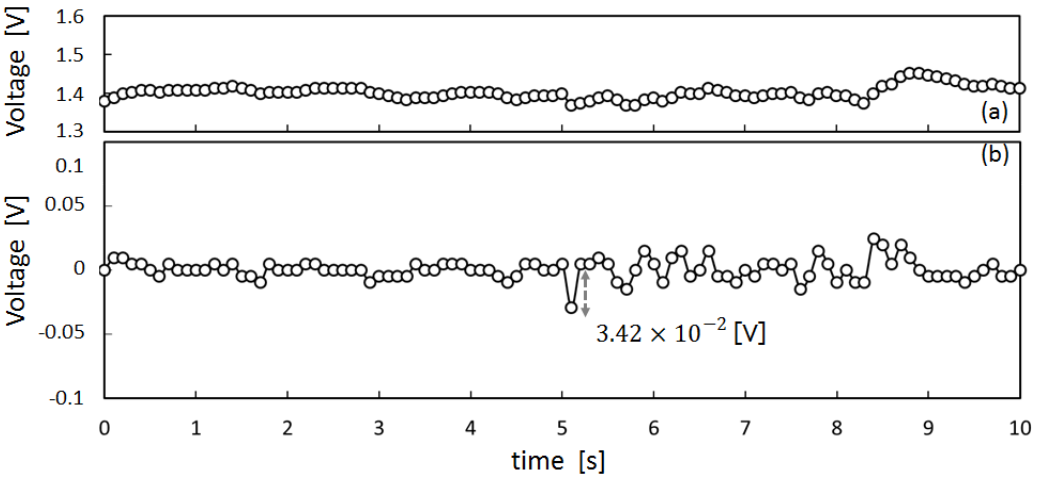

Figure 2.5. Ear-canal movement of conversation: (a) shows the measured values for movement of the ear canal during conversation; (b) shows the amount of change in these measured values. The amount of change was obtained by subtracting the immediately anteceding measured value (100 ms before obtaining the measurements because measurements are performed at 10 Hz) from the current measured value.

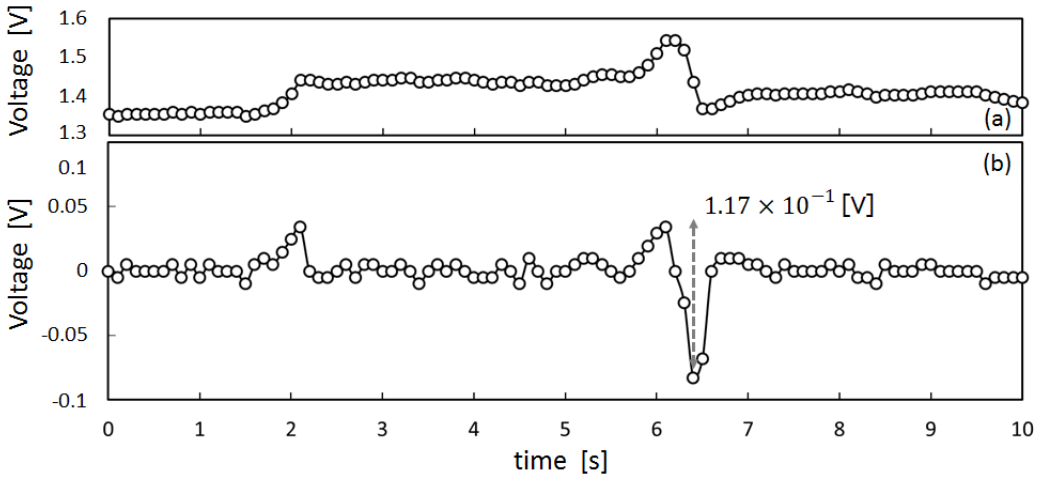

Figure 2.6. Ear-canal movement of yawn: (a) shows the movement of the ear canal during yawning, while (b) shows the corresponding amount of change.

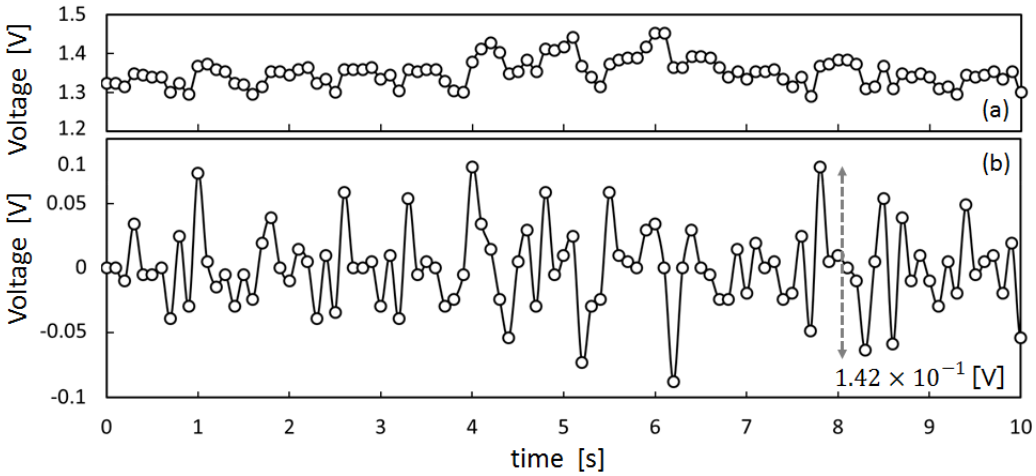

Figure 2.7. Ear-canal movement of chewing: (a) shows the movement of the ear canal during chewing of gum, while (b) shows the corresponding amount of change.

In this study, I used the fact that shape changes to the ear canal persist longer than changes due to facial expressions during chewing to estimate meal times. I aimed for an accuracy of within five minutes and used the newly defined "Meal Quality Feature (MQF)" for meal time estimation. The MQF is determined by obtaining the absolute value of the amount of change based on shape changes to the ear canal and calculating the sum of the mean and standard deviation of this absolute value within a certain period. During eating, the ear canal changes in shape considerably more than during facial expressions as a result of chewing. Because this change is continuous, the MQF of the time spent eating is greater than the MQF of the time spent not eating. A threshold is introduced to determine the size relationship of the calculated MQF. Shape changes to the ear canal differ among individuals, which results in a different MQF value being calculated for each subject. In this study, a threshold that differs depending on the subject was introduced instead of a uniquely determined threshold. The threshold was 50% of the difference between the maximum (max) and minimum (min) MQF calculated for each subject. The time during which the MQF continues to remain above the threshold is the meal time. The

MQF is calculated by grouping the measured values into five-minute intervals, such that the estimated meal time includes approximately five minutes of error. The details of the meal time estimation algorithm are written below. Furthermore, while the sensor is worn and used in both ears, this algorithm is capable of estimating meal times using only the sensor information obtained from either the left or right ear

Step 1. The mealtime estimation interval $t_{interval}$ is set at 5 min (i.e., 300 s). The sampling frequency f of the 10-bit analog to digital (AD) converter used in the measurements is set at f = 10 Hz. This is because chewing involves a constant cycle of repetitive, alternate contractions of the mouth's opening and closing muscles within the frequency range of 1.1–1.7 Hz [38].

Step 2. The sensor wearing time t_{wear} is at first decided, and then shape changes to the ear canal are measured for t_{wear} (seconds) by the sensor shown in Figures 2.3 and 2.4. The measured values are converted to measured data using $\boldsymbol{a} = \{a_1, a_2, \ldots, a_n\}$ (unit: V), where n represents the number of data measurements, and $n = t_{wear} \times f$. For example, when a subject wears the sensor for two hours a day (t_{wear} = 7200 s), $n = 7200 \times 10 = 72000$.

Step 3. Outlying values included among the measured data $\boldsymbol{a}$ are found. The overall mean of the measured data $\boldsymbol{a}$ is determined. Then 130% and 70% of this overall mean are set as the upper limit S_u and lower limit S_l, respectively, to establish a tolerance range $[S_l, S_u]$. Considering measured data a_i (i = 1, 2, . . . ,n) outside the range $[S_l, S_u]$, all values within one second before and after this range $\{a_{i-5}, \ldots, a_i, \ldots, a_{i+5}\}$ are set as outlying values. The identification of outlying values helped to eliminate sensor signals with an amplitude greater than that of chewing, which were observed during the removal of the earphone-type sensor and readjustment its position. It also

allowed for the elimination of signals with an amplitude smaller than that of chewing, which were observed during vibration of the sensor cable.

Step 4. The absolute value c_i of the amount of change in the shape of the ear canal is determined using Equation (2.1) and is set as the data for the amount of change $\boldsymbol{c} = \{c_1, c_2, \ldots, c_i, \ldots, c_n\}$.

$$c_i = \begin{cases} |a_{i+1} - a_i| & \text{if neither } a_i \text{ nor } a_{i+1} \text{ is an outlying value} \\ \text{"outlying value"} & \text{otherwise} \end{cases} \quad (2.1)$$

Step 5. The calculated data $\boldsymbol{c} = \{c_1, c_2, \ldots, c_n\}$ is divided into $\{\boldsymbol{b}_1, \boldsymbol{b}_2, \ldots, \boldsymbol{b}_j, \ldots, \boldsymbol{b}_p\}$, where $p = t_{wear} / t_{interval}$, and the number of elements included in each $\boldsymbol{b}_j$ (called n') is given by $n' = n/p$. In this case, $\boldsymbol{b}_j = \{c_{min(j)}, c_{min(j)+1}, \ldots, c_{max(j)-1}, c_{max(j)}\}$, where $min(j) = (j - 1) \times n'$, and $max(j) = j \times n'(j = 1, 2, \ldots, p)$.

For example, when a subject wears the sensor for two hours per day (t_{wear} = 7200 s), p = 7200/300 = 24, and n' = 72000/24 = 3000. As a result, the calculated data $\boldsymbol{c} = \{c_1, c_2, \ldots, c_{72000}\}$ is divided into $\{\boldsymbol{b}_1, \boldsymbol{b}_2, \ldots, \boldsymbol{b}_{24}\}$, where $\boldsymbol{b}_1 = \{c_1, c_2, \ldots, c_{3000}\}$, $\boldsymbol{b}_2 = \{c_{3001}, c_{3002}, \ldots, c_{6000}\}$, . . ., and $\boldsymbol{b}_{24} = \{c_{69001}, c_{69002}, \ldots, c_{72000}\}$.

Step 6. The mean $\bar{c}_j$ and standard deviation σ_j of the elements in each $\boldsymbol{b}_j$ (except outlying values) are calculated, and Equation (2.2) is used to find the sum d_j of these values and set as the MQF $\boldsymbol{e}_q = \{d_1, d_2, \ldots, d_j, \ldots, d_p\}$.

$$d_j = \bar{c}_j + \sigma_j \quad (2.2)$$

Chewing is characterized by greater and continuously changing amplitude. Taking the absolute value of the amount of change and the sum of its mean value and standard deviation produces a larger value for d_j during chewing (greater amplitude indicates a larger mean value and continuous changes in amplitude result in a larger standard deviation).

Step 7. The maximum and minimum MQF are found, and the mean of these two values is set as the threshold. The time during which the MQF is above the threshold represents the mealtime.

For example, when a subject wears the sensor for two hours per day from 11 a.m. to 1 p.m., the MQF d_1 corresponds to 11:00–11:05, the MQF d_2 corresponds to 11:05–11:10, and the MQF d_{24} corresponds to 12:55–13:00.

Notice that there exists neither threshold training nor a testing phase in this mealtime estimation algorithm. The threshold for determining whether it is the mealtime or not is always an unknown parameter before executing the algorithm, and it is adaptively calculated at step 7 without prior knowledge about the subject's personal information. Thus, the threshold differs each time a user wears the sensor regardless of whether or not he or she is the same person. On the other hand, the algorithm is based on the assumption that the measured data will always include mealtimes. A training phase to learn the threshold in advance may be necessary to accurately estimate mealtimes, even for cases in which this prerequisite is not satisfied.

2.2.3 Data collection protocol

The following two experiments were performed to confirm if meal times could be measured by the proposed method and if eating could be differentiated from running.

The first experiment was designed to demonstrate the usefulness of the proposed method (sensor and meal time estimation algorithm) for estimating meal times. The subjects of this experiment comprised one woman and six men, all healthy individuals aged 22 years, who were labeled as subjects A to G. These subjects wore

the sensor in Figure 2.3 in their right ear for two hours a day (11 a.m. to 1 p.m.) and also wore a small PC on their body to record voltages from the sensor and the times of these voltages. The subjects were then asked to spend their daily lives freely without any restrictions in their activities (e.g., eating, conversations, walking, climbing stairs, using a computer, or using a smartphone, removal and insertion of an earphone-type sensor). Once the experiment ended, the subjects were asked to answer a questionnaire about their meal start and end times during the experiment. Moreover, because the sensor used in the experiment has almost the same shape and weight as an ordinary, commercially-available earphone, no discomfort is experienced from the long-term wear of the sensor. The measurement time in this experiment, however, was set at 2 h to minimize subjects' time constraints. This experiment was performed during lunchtime hours (from 11 a.m. to 1 p.m.) to accurately evaluate the utility of the meal time estimation algorithm.

The second experiment was designed to investigate if chewing could be differentiated from running. The subjects of this experiment included four fit and healthy men with good dentition and a mean age of 22.8 years (±0.75 years) and 43 years who were labeled as subjects H to K. Shape changes to the ear canal were measured during chewing and running in these four subjects, and the correlation coefficient of shape changes to the ear canals of the left and right ears was determined. In this experiment, the subjects were asked to wear the sensor presented in Figure 2.3 in both ears. The subjects also wore a small PC on their body to record the voltages from the sensor and the times of these voltages.

Full explanations of the content and purpose of these experiments were provided to the subjects, who then provided their written informed consent to participate. The personal information of the subjects obtained from these experiments

was strictly managed and was not used for any purpose other than that to which the subjects consented.

2.3 Results

Table 2.1. Experimental results of meal time measurements. The results of the questionnaire and meal time estimation algorithm for subjects A to G are presented in Table 2.1. Table 2.1 also shows the ratio of overlap between meal times from the results of the questionnaire and the meal time estimation algorithm. The ratio of overlap is defined as "the ratio of the logical product of both intervals (interval from the questionnaire and interval from the estimation algorithm) to the logical sum of both intervals."

Subject	Questionnaire results [h:m]	Estimated results [h:m]	%Overlap
A	12:14–12:30	12:20–12:30	5/8
B	12:12–12:21	12:15–12:25	6/13
C	12:10–12:18	12:15–12:20	3/10
D	12:06–12:20	12:10–12:20	5/7
E	12:20–12:37	12:25–12:40	3/5
F	12:35–12:52	12:40–12:55	3/5
G	12:24–12:29	12:25–12:30	2/3

The results of the questionnaire and meal time estimation algorithm for subjects A to G are presented in Table 2.1. Table 2.1 also shows the ratio of overlap between meal times from the results of the questionnaire and from the meal time estimation algorithm. The ratio of overlap is defined as "the ratio of the logical product of both intervals (interval from the questionnaire and interval from the estimation algorithm) to the logical sum of both intervals." For example, in the case of subject B, the interval obtained from the questionnaire was from 12:12 to 12:21, whereas the interval obtained from the meal time estimation algorithm was from

12:15 to 12:25. In this case, the logical product of both intervals is an interval from 12:15 to 12:21, and the logical sum between both intervals is an interval from 12:12 to 12:25. The ratio of overlap is therefore 6/13 (= [12:15–12:21]/[12:12–12:25]).

In addition, the MQF of subject A calculated using the meal time estimation algorithm is presented in Figure 2.8. The vertical axis in Figure 2.8 shows the MQF in volts (V), while the horizontal axis shows the time (11 AM to 1 PM) in hours and minutes (h:m). The time during which the MQF is above the threshold is TIME1, while the time during which the MQF is below the threshold is TIME2. TIME1 is the estimated meal time. The mean value for the MQF in TIME1 is Mean1, and the mean value for the MQF in TIME2 is Mean2. From Figure 2.8, TIME1 of subject A was from 12:20 to 12:30 and Mean1 and Mean2 were 1.06×10^{-1} V and 1.49×10^{2} V, respectively. TIME1, Mean1, and Mean2 of all subjects were determined by the same method as determined in subject A and are presented in Table 2.2. When the actual meal times of all subjects obtained by the questionnaire were compared with the estimated meal times (TIME1) obtained by the algorithm, the differences for each subject fell within a range of five minutes. From Table 2.2, it is evident that the largest Mean1 was in subject A, at 1.06×10^{-1} V, while the smallest Mean1 was in subject B, at 1.31×10^{-2} V, revealing individual differences in Mean1 values. These results indicate that despite individual differences among subjects, the variability between the questionnaire results and estimated results fell within the pre-set range of accuracy (within five minutes) for all subjects, and the meal time estimation algorithm was capable of correctly estimating meal times within the scope of the experiment.

Table 2.2. Experimental results. The mean value for the MQF in TIME1 is Mean1, and the mean value for the MQF in TIME2 is Mean2.

Subject	Mean1 [V]	Mean2 [V]
A	1.06×10^{-1}	1.49×10^{-2}
B	1.31×10^{-2}	5.42×10^{-3}
C	8.21×10^{-2}	1.39×10^{-3}
D	3.15×10^{-2}	8.20×10^{-3}
E	3.05×10^{-2}	9.05×10^{-3}
F	5.82×10^{-2}	6.90×10^{-3}
G	7.20×10^{-2}	9.90×10^{-3}

I next determined Pearson's product–moment correlation coefficient (hereafter referred to as "correlation coefficient") from the measured shape changes to the left and right ear canals during running and chewing gum in subjects H to K, which are presented in Table 2.3. In addition, Figures 2.9 and 2.10 show the measured shape changes to the left and right ear canals during running and chewing for subject H. The vertical axes in Figures 2.9 and 2.10 show the output voltage from the sensor in volts (V), while the horizontal axes show the time in seconds. In Table 2.3, data for subjects H to K are listed, and the largest correlation coefficient r was 0.941 for subject J and the smallest coefficient r was 0.741 for subject I during running. In contrast, during gum chewing, the largest correlation coefficient r was 0.384 in subject J and the smallest coefficient r was 0.175 in subject K. Figures 2.9 and 2.10 also show that the left and right measured values are almost synchronized during running, whereas they are not synchronized during chewing. Therefore, Table 2.3 and Figures 2.9 and 2.10 reveal a strong correlation in the measured results for the left and right ear canals during running but not during chewing. A clear difference was observed in the correlation coefficients of the measured results for the left and right ear canals during running and chewing within the scope of this experiment.

Table 2.3. Correlation coefficients of shape changes to the left and right ear canals (similarity of shape changes to the left and right ear canals)

Subject	Running	Chewing
H	0.796	0.221
I	0.741	0.359
J	0.941	0.384
K	0.757	0.175

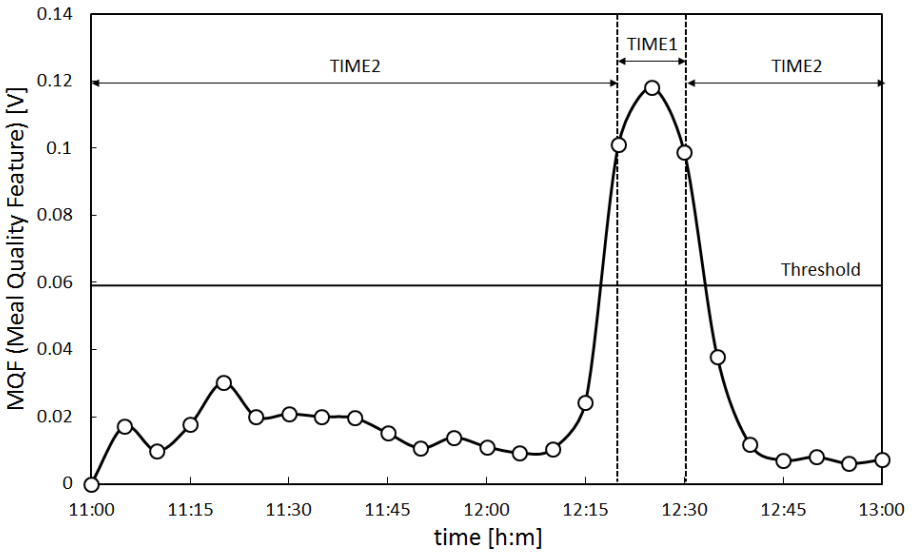

Figure 2.8. Meal quality feature of subject A. The MQF of subject A calculated using the meal time estimation algorithm is presented in the figure. The vertical axis in the figure shows the MQF in volts (V), while the horizontal axis shows the time (11 a.m. to 1 p.m.) in hours and minutes (h:m). The time during which the MQF is above the threshold is TIME1, while the time during which the MQF is below the threshold is TIME2. TIME1 is the estimated meal time.

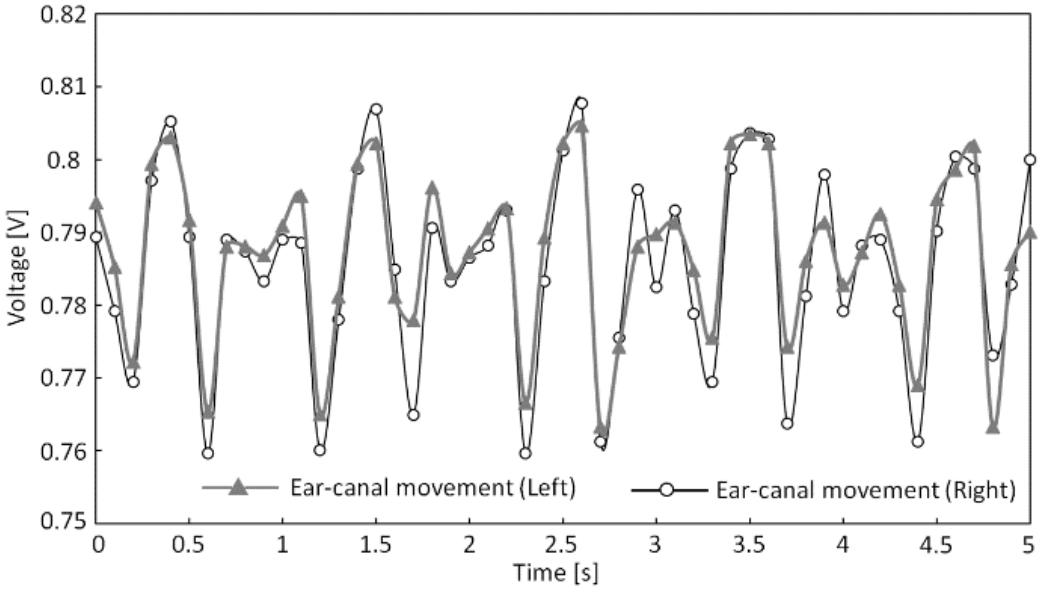

Figure 2.9. Right and left ear canal movement during running (subject H)

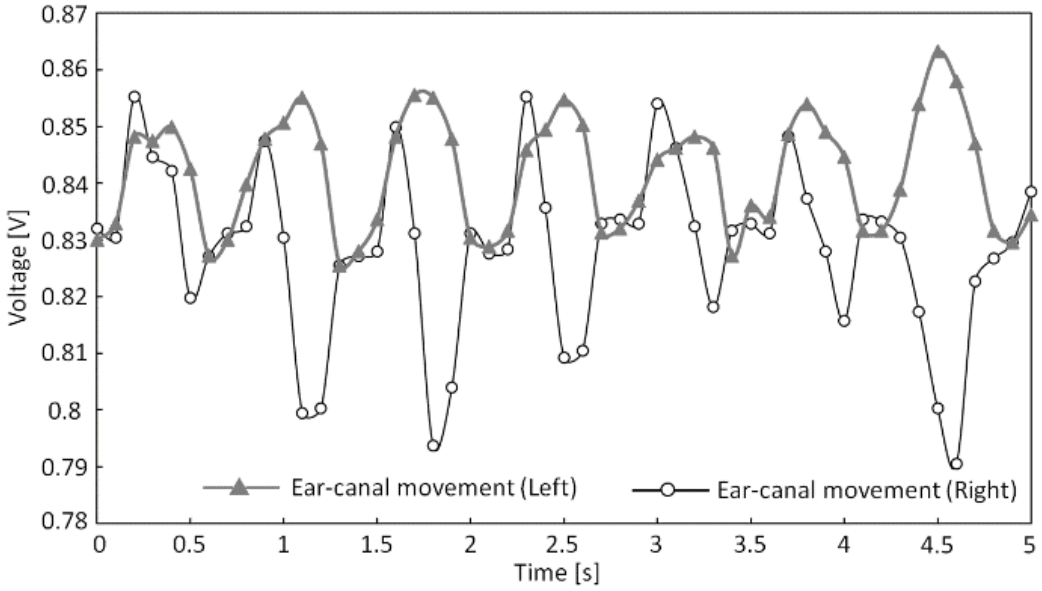

Figure 2.10. Right and left ear canal movement during chewing (subject H)

2.4 Discussion

Based on the experimental results, I first discuss whether the proposed method can estimate meal times (food intake) and differentiate eating (chewing) from running.

I can conclude that this sensor and algorithm can be used to estimate meal times within the scope of my experimental results. This is because the difference between the actual and estimated meal times (TIME1) fell within five minutes for all subjects in my experimental results and Mean2 was less than 50% of Mean1. This demonstrates that meal times can be estimated regardless of individual differences in the shape changes to the subjects' ear canals using this sensor and algorithm. An error of up to five minutes nevertheless exists between the actual meal times and those estimated using this algorithm. This error is valid because MQF is defined as five minutes in the algorithm used in this study. If it was necessary to estimate the meal times to a higher degree of accuracy less than five minutes, a solution could be found by changing the time to calculate the MQF in accordance with the required accuracy. However, it is not theoretically possible to reduce the error to zero because this algorithm uses statistical processing.

Next, I discuss the impact of individual differences in shape changes to the ear canal on the meal time estimation results. All subjects had large MQF values for the actual meal times; however, these values differed for each subject. When the experimental results for Mean1 were compared between the seven subjects, I observed the largest Mean1 in subject A, at 1.06×10^{-1} V, and the smallest Mean1 in subject B, at 1.31×10^{-2} V. This difference in these values can be indicative of the effect of individual differences in shape changes to the ear canal. The MQF is calculated from the sum of the mean and standard deviation of the amount of change

based on the output voltage of the sensor. When the MQF is high, the mean and standard deviation for the amount of change are also large, which in turn indicate a substantial change in the distance between the sensor and eardrum. Thus, the MQF is large when the subject's ear canal movement is large. In case of this experiment, subject A exhibited the largest shape change to the ear canal, while subject B exhibited the smallest. Shape changes to the ear canal differ according to each individual, and these individual differences directly influence the MQF. However, the MQF of TIME1 was more than two-times larger than that of TIME2 for all subjects, indicating a clear difference between TIME1 and TIME2. These results suggest that meal times can be estimated within the range of error by setting a threshold based on the maximum and minimum MQF values of each subject. This is also performed in this algorithm, without being influenced by individual differences in shape changes to the ear canal. In the future, I aim to improve the accuracy of this algorithm by continuing to study meal time windows (e.g., meal times ranging from 5 min to 1 min).

I next discuss if chewing (eating) can be differentiated from running. I found that this sensor can be used to differentiate eating from running within the scope of my experimental results. This is because the measured results for the left and right ear canals during running strongly correlated with each other, whereas the results during chewing did not. If these activities are categorized based on correlation coefficients, they can be distinguished from each other. In particular, the measured waveforms of the left and right ear canals during running are similar, as shown in Figure 2.6, whereas measurements during chewing are not similar between the left and right ear canals. Table 2.3 shows that the correlation coefficient r during running was 0.941 at its highest and 0.741 at its lowest. Meanwhile, the correlation coefficient r during chewing was 0.384 at its highest and 0.175 at its lowest. Therefore, these

findings suggest that this is a viable method for using a single (fixed) threshold to differentiate eating from running, in marked contrast with the mealtime estimation algorithm, which adaptively varies the threshold every time a user wears the sensor. For example, running is identified when the correlation coefficient r calculated from the measured results of shape changes to the left and right ear canals exhibits a strong correlation equal to or greater than 0.7. In contrast, eating is identified when the correlation coefficient r exhibits no correlation or a weak correlation equal to or lower than 0.4 and when the meal time estimation algorithm identifies eating.

I now further discuss running and chewing based on the data presented in Figures 2.6 and 2.7. The running waveform in Figure 2.6 shows that the left and right ear canal waveforms are similar during running. On the other hand, the chewing waveform in Figure 2.7 reveals that the left and right ear canal waveforms differ during chewing. This indicates that during running, the same waveform resulting from running is superimposed onto the measured results for the left and right ear canals. The reason for this superimposition of the waveform onto the measured results is due to vibrations generated by the foot. The vibrations that occur when the foot makes contact with the ground are transmitted to the ear via the body and are consequently measured by the sensor. Running involves one foot at a time making contact with the ground; however, the same running waveform is superimposed onto the measured results for shape changes to the left and right ear canals. This is because the transmission pathways of the vibrations generated by the feet are the same. The pathways by which the vibrations that occur when the feet make contact with the ground are transmitted to the ears differ between the left and right feet from the soles of the feet up to the hips. However, from the hips to the lower back, chest, neck and head, vibrations arrive via the same pathway, regardless of the foot from which they originated. This is why transmitted vibrations are not biased toward any side and why

running leads to the same results being superimposed onto the measured results for shape changes to the left and right ear canals. Therefore, the measured results for shape changes to the left and right ear canals associated with running are similar. In contrast, the measured results for shape changes to the left and right ear canals associated with chewing are not the same, as evident in Figure 2.7. Chewing causes the temporal muscles to stretch and contract, which results in movement of the ear canal. If shape changes to the left and right ear canals associated with chewing were the same, the temporal muscles would expand and contract at the same time and in the same manner. Furthermore, if the left and right temporal muscles were to expand and contract at the same time and in the same way as a result of chewing, the jaw would move precisely up and down. However, the actual jaw movement during chewing is biased toward either the left or right. Because the left and right temporal muscles do not expand and contract at the same time or in the same way, shape changes to the ear canal associated with chewing differ between the left and right sides. Based on the above findings, I intend to estimate the amount of movement by analyzing the waveforms during running. In addition to estimating the amount of movement, I am currently conducting pulse measurements within the ear canal by using my proposed method and the same type of optical sensor. If I can estimate the amount of movement and improve the accuracy of pulse measurements, I can create a device capable of supporting a healthy lifestyle among users regarding exercise and diet by simply obtaining measurements from one the optical sensor inserted into the left and right ear canals.

2.5 Conclusion

In this chapter, I described a method for estimating meal times based on temporal changes in the amount of light received by a small optical sensor composed of an LED and a phototransistor inserted in the right ear canal. The device shines light toward the inner ear canal and receives light reflected back by the ear canal. An experiment performed using seven subjects was successful in estimating meal times in all subjects within a set range of error. Furthermore, an analysis of the measured values during running and chewing obtained from the same sensor inserted into the left and right ear canals of four subjects revealed that measurements from the left and right ear canals were strongly correlated during running, but not correlated during chewing. These findings allow running and chewing to be differentiated based on correlation coefficients.

In the future, I intend to develop a method for estimating the amount of movement of the body by analyzing waveforms during running. In addition to improving my meal time estimation algorithm and continuing to investigate methods for differentiating running and chewing, I aim to conduct further experiments using larger subject samples. I also hope to establish a method for measuring the pulse within the ear canal using my proposed method and the same type of optical sensor. Among the research on detecting chewing sounds via the ear, there is a study that used a microphone worn in the ear to sense chewing sounds transmitted through the bone [39]. More accurate meal time measurements might be achieved by combining the results of my study with those from the study that used a microphone. By combining all these research results, I aim to develop a device capable of supporting a healthy lifestyle of users regarding both exercise and diet.

Chapter 3:

A basic study for estimation of occlusal force using an earphone type sensor

3.1 Introduction

The number of the elderly is growing steadily, which spurs demand for monitoring technologies regarding dental occlusion and chewing. Chewing ability of the elderly is reported to greatly contribute to longer health expectancy [13, 15]; moreover, epidemiological studies say that chewing ability in the elderly is closely related not only to the body, but also to mental activities and even vital functions [16]. I have been engaged in development of wearable devices that can easily measure chewing ability at home or in hospital, and in research on health management using thus measured results. In Chapter 2, I aimed mainly at health care and monitoring and focused on distinctive variation patterns that appear only in eating (chewing); I implemented mealtime measurements using an ear wearable sensor [40]. In that research, I evaluated accuracy of meal duration by means of average overlap ratio. Assumed, for example, that actual meal lasted from 12:12 through 12:21, while the time measured by the wearable sensor was from 12:15 through 12:25; then the logical product is 12:15 through 12:21, while the logical sum is 12:12 through 12:25. Thus, overlap ratio is 6/13 (= [12:15 – 12:21]/[12:12 – 12:25]). In that research, average overlap ratio in seven subjects was 0.567. As a next step in chewing evaluation, I continue research in occlusal force measurement.

Conventional methods of occlusal force measurement include those using an intramouth sensor [41–43] and those estimating occlusal force from muscle potential acquired by electrodes attached to the jaw and cheeks [44]; the former measure occlusal force when only a sensor is put in the mouth, while the latter measure chewing muscle activity during daily activities including eating as well as nocturnal sleep, and appropriate measuring devices are used in both cases.

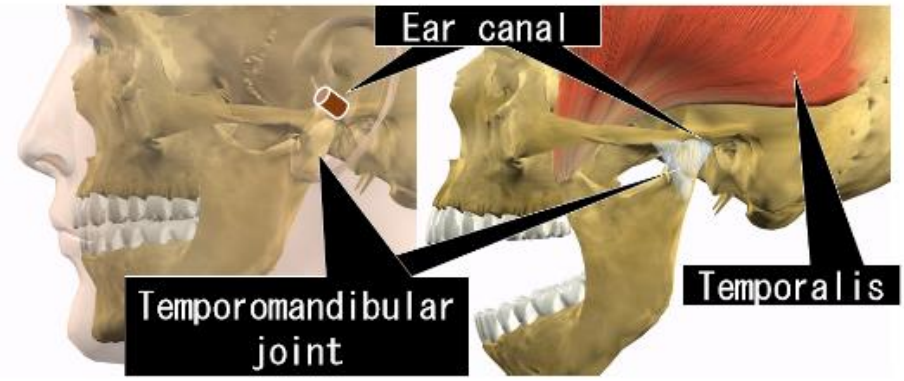

Figure 3.1. Anatomical positional relationship between the ear canal, temporal muscle (temporalis).

As distinct from the previous research, I and co-researcher aim at developing a device that makes possible simple monitoring of occlusion and chewing during meals by common users who have no specialized knowledge. Such monitoring device would be useful, for example, to improve nutrition procedures in postoperative gastric cancer patients [18, 45]. Patients who underwent gastrectomy for cancer are at high risk of malnutrition because of decline in gastric accommodation and emptying [17]. In order to avoid malnutrition, doctors need a device to monitor occlusion and chewing so as to instruct patients towards better nutrition procedures. Occlusal force is produced by the temporalis and the temporomandibular joint. The anatomical relation between the temporalis and the temporomandibular joint is illustrated in Figure 3.1; occlusion results in a change of shape of the ear canal adjacent to the temporalis and the temporomandibular joint. I am working on occlusal force measurement through estimating meal duration and chewing count using an ear wearable sensor, based on the knowledge of the ear canal deformation due to occlusion.

This study is intended to measure occlusal force using a simple device (an ear wearable sensor combined with a small microcontroller) that is free of intramouth

sensors (which makes possible measurement during eating), and does not impede movement of chewing muscles (cheek joint, temporalis, etc).

As the first report on my R&D in occlusal force measuring device, this chapter presents discussion and experimental results about whether occlusal force can be estimated from correlation between occlusion force and movement of the ear canal.

3.2 Methods

3.2.1 Overview of experiments

The experiments were intended to examine correlation between occlusal force and ear canal movement, and to confirm whether occlusal force can be estimated from ear canal movement. For this purpose, I developed a system that can simultaneously measure occlusal force and ear canal movement (see Section 3.2.2, Figure 3.2). When developing the experimental system, I first fabricated a prototype of occlusal force sensor. Then I experimentally determined characteristics of the sensor (see Sections 3.2.4.1 and 3.3.1). As regards measurement of ear canal movement, I used an ear wearable sensor that I have worked on Chapter 2.

3.2.2 Experimental system

The experimental system fabricated for this study is shown in Figure 3.2. In this system, analog signals measured by an occlusal force sensor (“a” in Figure 3.2) and earphone-type sensor (“b” in Figure 3.2) are converted in digital signals by AD

converter at sampling frequency of 10 Hz and resolution of 12 bit; the digital signals are recorded to a storage device together with timestamps.

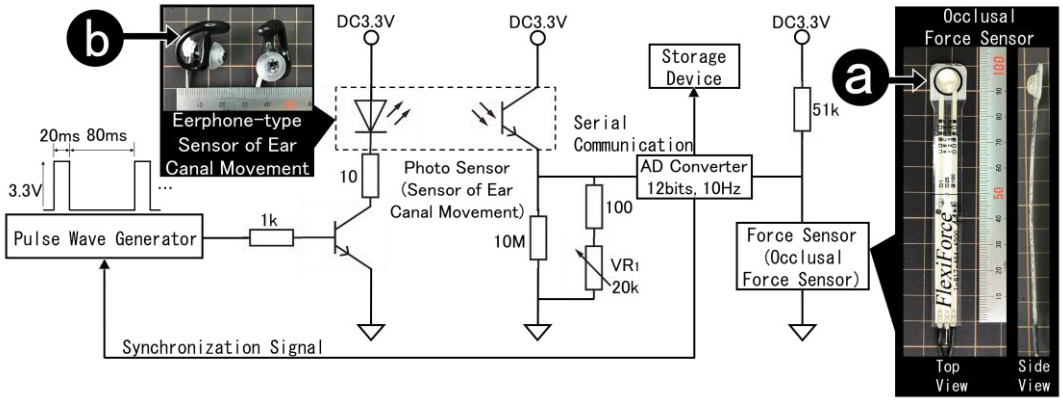

Figure 3.2. Electronic circuit around the sensor.

The occlusal force sensor was fabricated using a pressure sensor (FlexiForce A201-100 by NITTA Corp., max. force: 440 N). This pressure sensor features output linearity within ±5% against applied pressure. A polyurethane resin hemisphere with diameter of 9.5 mm and height of 3.8 mm was bonded at the pressure sensing area (a circle of 9.5 mm in diameter near the tip of arrow “a” in Figure 3.2). Besides, a 0.63-mm thick polypropylene sheet was bonded to the backside of the sensing area. The sensor measures occlusal force when the second molar teeth occlude, the polyurethane resin hemisphere and the polypropylene sheet being placed at the upper and lower jaw, respectively. The hemispheric piece is to evenly transmit the force (point load) applied from the upper jaw across the sensing area; the sheet is to protect the sensing area from the teeth. A signal cable is connected to the opposite end of the sensing area (bottom of the photograph on the right of Figure 3.2).

The ear wearable sensor has the shape of an inner earphone with a built-in optical sensor (QRE1113 by Fairchild Semiconductor). The optical sensor houses an infrared LED and a phototransistor; the LED illuminates the ear canal, and reflected light is received by the phototransistor to measure movement of the ear canal when

the teeth are clenched (see Figure 3.3). In this optical sensor, output grows with the amount of light reflected from an object, and vice versa. Output offset voltage of the optical sensor can be adjusted via the variable resistor VR_1. The tip of the ear wearable sensor inserted into the ear canal is made with reference to a commercial M-size earphone.

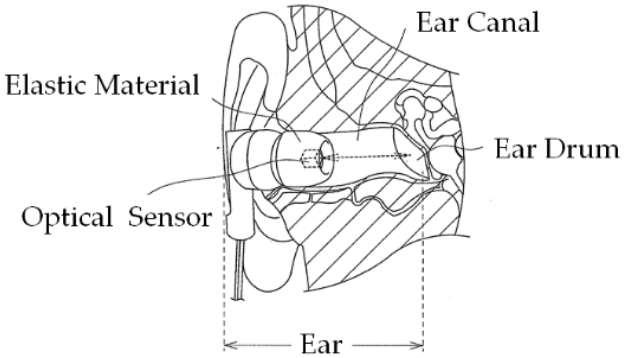

Figure 3.3. Measurement principle for changes in the shape of the ear canal.

The LED is provided with a pulse wave generator to control light emission. This pulse wave generator is synchronized with the AD converter connected to the ear wearable sensor. Thus, the light is only emitted during AD conversion to enhance LED emission. As a result, the influence of ambient infrared light transmitted via the skin near the outer ear can be suppressed, and one can expect for higher S/N ratio. The AD converter and pulse wave generator were implemented using a single microcontroller (mbed LPC1768 by NXP Semiconductors) and proprietary software. Used as the storage device was a notebook PC (CF-B11QD3BP by Panasonic, Windows 10 Pro Ver. 1703). The microcontroller and PC were connected via USB; communication was implemented by RS-232 specification using a freeware (CoolTermWin Ver. 1.4.7).

3.2.3 Subjects

The subjects were six young healthy persons (males aged 21 to 27, average age: 23.3) denoted by A, B, C, D, E, and F. The subjects were able to clamp the occlusal force sensor with their second molar teeth without any trouble (no symptoms of pain or fatigue in the teeth and the jaw). Those wearing dental braces, etc and those who felt uncomfortable with the ear wearable sensor were excluded.

Besides, this study was approved by the Shinshu University Human Research Ethics Committee; after being explained about the contents of experiments, the subjects signed a written consent.

3.2.4 Experimental methods

3.2.4.1 Measurement of characteristics of occlusal force sensor

The occlusal force sensor is paced, the hemispheric piece up and the sheet down, on a horizontal table that can withstand a load of 200 N per square centimeter; then the sensor output (AD converted value) is measured while a downward force from 0 through 60 N is applied normally at the center of the hemispheric piece. The load was applied to the occlusal force sensor using a digital force gage (ZP-200N by Imada Inc.).

3.2.4.2 Correlation between outputs of occlusal force sensor and ear sensor

This experiment examined correlation between chewing and movement of the ear canal. As the occlusal force sensor was clamped by the second molar teeth, results of both ear wearable sensor and occlusal force sensor were measured and recorded. In this experiment, each of six subjects performed five runs. A subject was seated in a chair with the wearable sensor attached to his right ear, and clamped the occlusal force sensor by the second molar teeth, the hemispheric piece up and the sheet down. The occlusal force sensor was inserted in the mouth from the end where the hemisphere and the sheet are installed, so that the end with the cable projects from the mouth. In this experiment, a subject gradually increases pressure on the occlusal force sensor for about 2 seconds to fix the sensor in the mouth, and then relax the pressure to return to the initial condition. For hygiene considerations, the sensor was wrapped with a thin (about 0.04 mm) polyethylene film during the measurement; after each measurement, the sensor was washed and disinfected by ethanol, and the polyethylene film was replaced. The ear wearable sensor was also washed and disinfected by ethanol after each measurement.

3.2.4.3 Estimation of occlusal force from ear canal movement

Among five runs if each subject in the experimental method of Section 3.2.4.2, the outputs of both sensors in the first through fourth runs were used as learning data, and the output of the ear wearable sensor in the fifth run was used as test data for estimation. Thus, estimated data were compared to the actual results of the fifth run. Besides, in order to eliminate offset components in the output of ear

wearable sensor in all runs, output variation with respect to the minimum value was determined for each subject in every run and then used in earning and estimation.

Two methods—least squares and weighted average—were used in the estimation. In estimation of the ear wearable sensor output by least squares, measured values of both sensor outputs in the first through fourth runs were linearly approximated by least squares.

On the other hand, the following expression was used for estimation by weighted average.

$$o_w = \frac{\sum_{i=0}^{n} w_i o_i}{\sum_{i=0}^{n} w_i} \tag{3.1}$$

Here o_i is measured value (occlusal force sensor output) in the first through fourth runs, w_i is weight applied to each measured value, and n is the total number of learning data. The weights w_i were obtained using the most typical Gaussian function shown below.

$$w_i = \mathrm{a} \exp\left(\frac{(x-b)^2}{2c^2}\right) \tag{3.2}$$

Here the weight is maximum for x_i =0; a=1 and b= 0 is set so that the weight is 1. The value of x_i was determined by Equation (3.3); the parameter c was set to the standard deviation of output variation of the ear wearable sensor in the fifth run.

$$x = \|A - B_i\| \tag{3.3}$$

Here A is output variation of the ear wearable ear sensor used to estimate output of the occlusal force sensor, and B_i (B_1 through B_n) is data set of output variation of the ear wearable ear sensor from the first through fourth runs.

3.3 Results

3.3.1 Results of measurement of occlusal force sensor characteristics

Figure 3.4 presents measured output (AD converted value) of the occlusal force sensor while the applied load is changed from 0 to 60 N in increments of 20 N. The approximation line and approximation expression shown in the diagram were derived by least squares. As can be seen from the graph, output of the occlusal force sensor varied in proportion to the applied load, thus showing one-to-one correspondence.

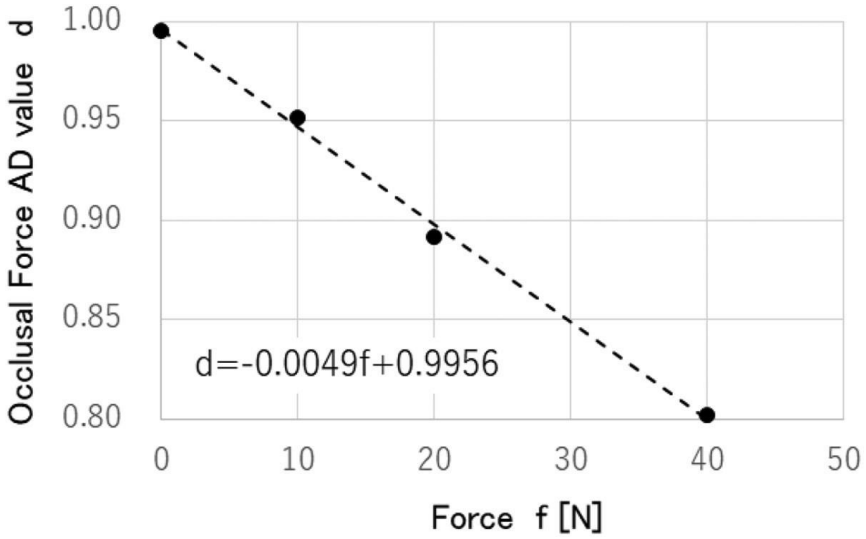

Figure 3.4. Measurement result of occlusal force sensor.

3.3.2 Results for correlation between outputs of occlusal force sensor and ear sensor

Average, maximum, minimum values and standard deviation of correlation coefficients between outputs of the occlusal force sensor and the ear wearable sensor obtained in five runs for subjects A through F are given in Table 3.1. When estimating

occlusal force with the ear wearable sensor, the average absolute value of correlation coefficient should be close to 1, and the standard deviation should be close to 0.

As can be seen from Table 3.1, average correlation coefficient for all subjects was above 0.89 in absolute value, and standard deviation was 0.030 or less. The correlation coefficient was positive for subjects A through D, and negative for subjects E and F. Subject B showed the greatest absolute value of correlation coefficient (minimum: 0.944, maximum: 0.961, average: 0.950, SD:0.028), while subject D showed the smallest value (minimum: 0.848, maximum: 0.921, average: 0.893, SD: 0.030).

Table 3.1. Correlation between output value of occlusal force sensor and output value of ear wearable sensor

Subject	Average	Maximum	Minimum	Standard deviation
A	0.918	0.953	0.896	0.02
B	0.950	0.961	0.944	0.03
C	0.906	0.930	0.861	0.03
D	0.893	0.921	0.848	0.03
E	–0.935	−0.915	−0.960	0.01
F	–0.931	−0.907	−0.966	0.02

The graph in Figure 3.5(a) shows measured results in which the correlation coefficient between outputs of the occlusal force sensor and the ear wearable sensor was the highest in five runs of subject A with positive correlation. Besides, similar graph for subject E with negative correlation is shown in Figure 3.5(b). Here the horizontal axis plots time, the left vertical axis plots occlusal force sensor output (AD converted value) and the right vertical axis plots ear wearable sensor output (AD converted value). These values measured every 0.1 second provide a quick overview of correlation between both outputs as well as outliers in the measured data.

As indicated by Figure 3.5 and Table 3.1, correlation between outputs of the occlusal force sensor and the ear wearable sensor can be positive or negative depending on the subject. Besides, correlation was either only positive or only negative in all five runs.

As shown in Figure 3.5, output spread of the occlusal force sensor in this experiment was about 0.2 (from 1.0 toward about 0.8). According to Figure 3.4, the output's change from 1.0 to 0.8 means that a force about 40 N was applied to the sensor. In this experiment, the subjects did not occlude their teeth strongly. Two reasons were given in their interviews. The first reason was that the hemispheric piece slipped, or felt like slip, when bitten, thus preventing the subjects from strong clenching. The second reason was that the hemispheric piece split (broke), or felt like about to break, when bitten, thus preventing the subject strong clenching.

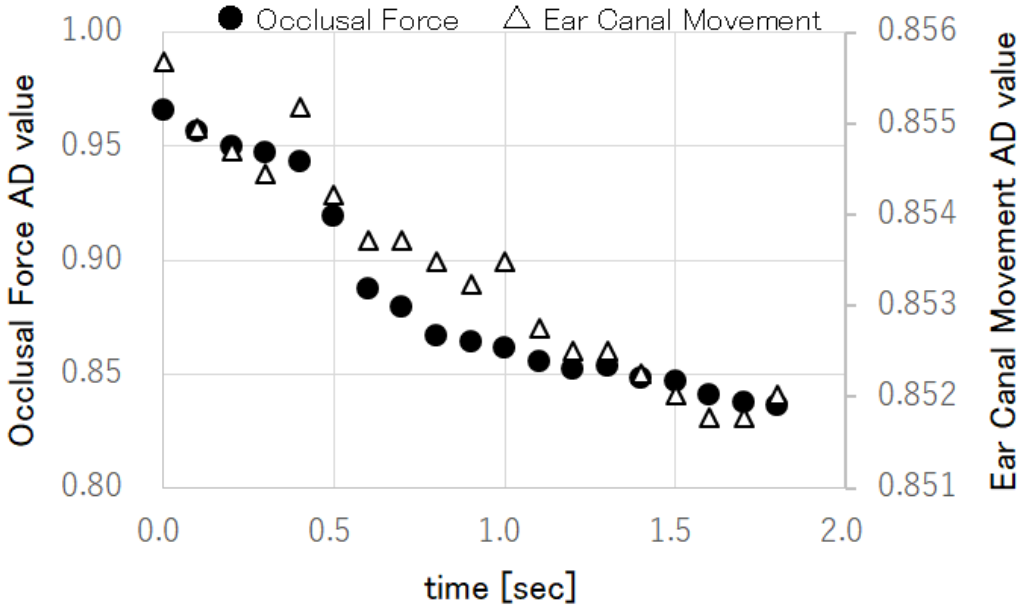

(a) subject A

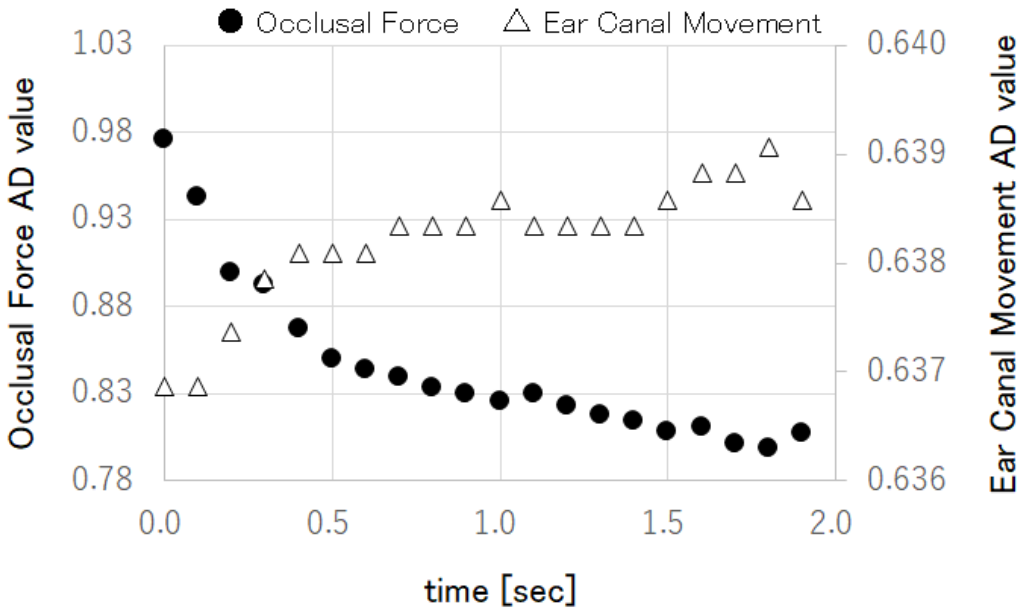

(b) subject E

Figure 3.5. Measurement results of occlusal force and ear canal movement.

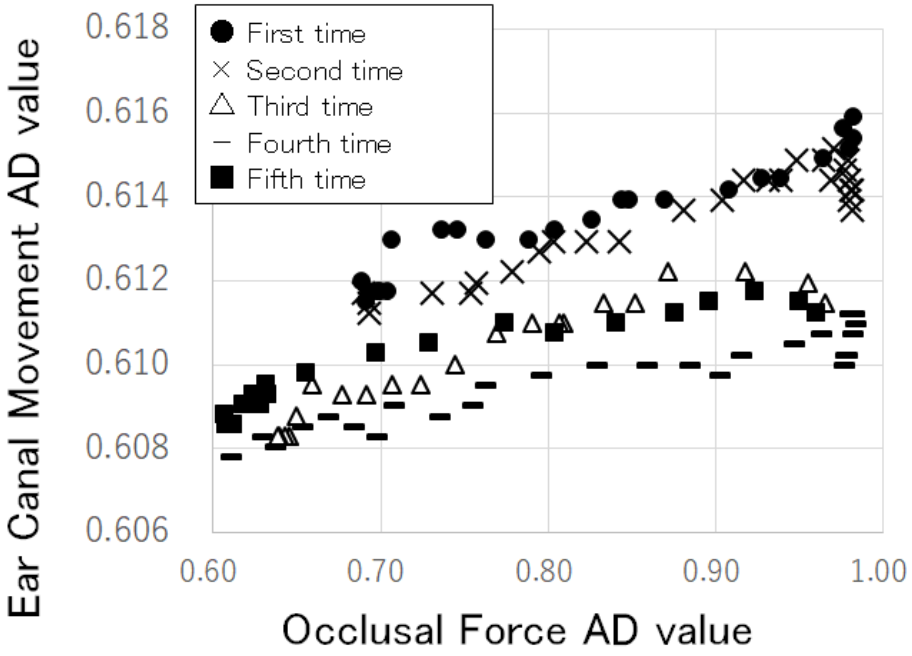

Figure 3.6. Five experiment results for subject B

Figure 3.6 shows superimposed results of five runs for subject B that showed the highest correlation. Here the horizontal axis plots occlusal force sensor output

(AD converted value), and the vertical axis plots ear wearable sensor output (AD converted value). The plot is indicative of repeatable correlation. A data spread along the vertical axis means low repeatability. All data in Figure 3.6 show positive proportional relation, that is, positive correlation.

3.3.3 Results for estimation of occlusal force from ear canal movement

Table 3.2 shows differences (average, standard deviation, standard error) between measured results and estimated results (least squares and weighted average) for subjects A through F. Here standard error is defined as standard deviation divided by the square root of each data. The measured results pertain to the fifth run; the data measured in the first through fourth runs were used for learning in estimation. The smaller are the average, standard deviation, and standard error, the higher is estimation accuracy. The smallest difference (the smallest values of average, standard deviation, standard error) was obtained in least squares estimation for subject E. On the other hand, the greatest difference was obtained in weighted average estimation for subject B. Comparing the estimation methods (weighted average and east squares), average difference was smaller with least squares estimation for all subjects. However, the difference was strongly affected by the measured results (values measured in the fifth run).

Table 3.2. Average value, standard deviation value, and standard error value of difference between measurement result and estimation result for each subject

Subject	Method	Average	Standard deviation	Standard error
A	Least square	0.028	0.02	0.005
	Weighted average	0.031	0.02	0.005
B	Least square	0.060	0.03	0.007
	Weighted average	0.081	0.04	0.009
C	Least square	0.030	0.02	0.004
	Weighted average	0.032	0.02	0.005
D	Least square	0.026	0.03	0.006
	Weighted average	0.033	0.03	0.006
E	Least square	0.018	0.02	0.003
	Weighted average	0.028	0.02	0.003
F	Least square	0.026	0.03	0.005
	Weighted average	0.053	0.02	0.003

Measured and estimated results for subjects A and E are presented in Figure 3.7. The horizontal axis plots variation of the ear variable sensor output normalized against the minimum value; the left vertical axis plots occlusal force output (AD converted value) corresponding to variation of the ear variable sensor output; the right vertical axis plots occlusal force corresponding to the sensor output derived from Figure 3.4 (see Section 3.3.1). Here subject A with positive correlation shows positive proportional relation, while subject E with negative correlation shows negative proportional relation.

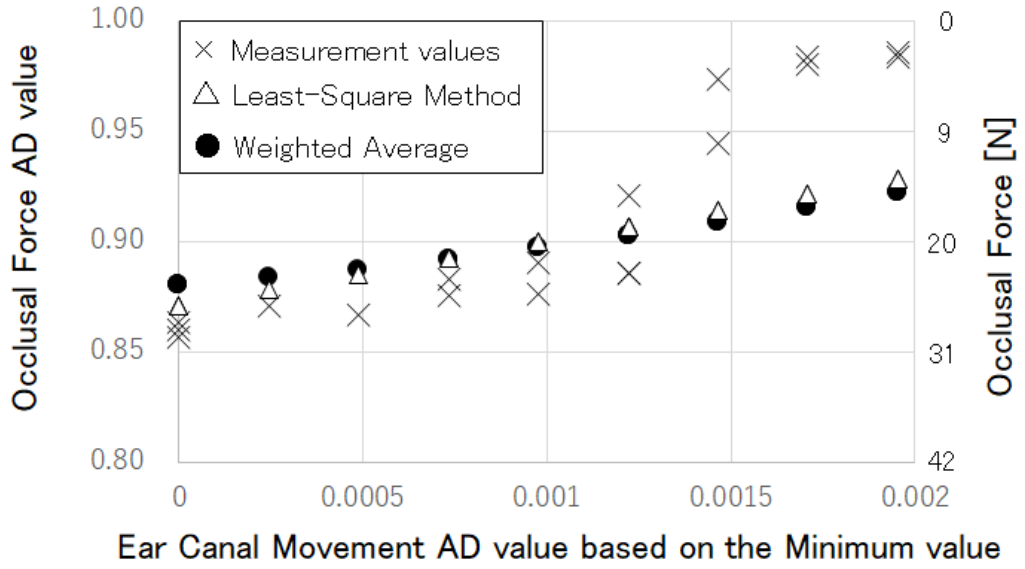

(a) subject A

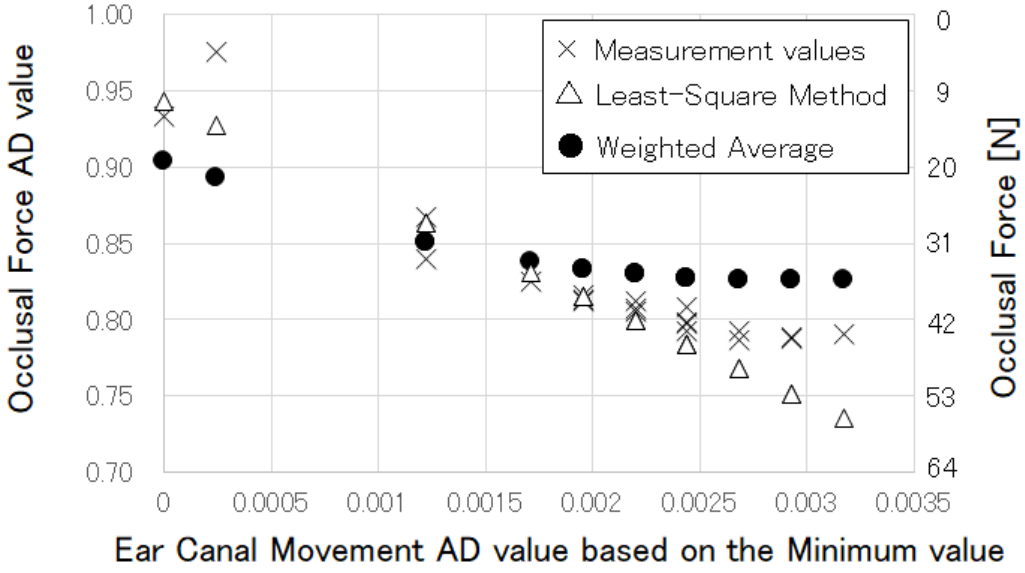

(b) subject E

Figure 3.7. Results of estimating occlusal force from ear canal movement.

In Figure 3.7, one can directly compare estimation by weighted average and by least squares. In Figure 3.7(a), both estimation methods produce almost same results, but results in Figure 3.7(b) are obviously different.

3.4 Discussion

The results of Figure 3.4 are indicative of one-to-one correspondence relationship between force and output of the occlusal force sensor, which means that the fabricated prototype sensor can be used in force measurement.

Occlusion conditions of subjects in the experiments can be understood from the results of Figure 3.4 and the output values in Figure 3.5. For example, subject A (Figure 3.5(a)) does not clench his teeth from 0 through 0.5 seconds, then performs clenching rapidly at 0.5 through 0.8 seconds, and after that, maintains the occlusal force on a certain level. Subject E (Figure 3.5(b)) rapidly clenches his teeth at 0 through 0.5 seconds, and then maintains the occlusal force on a certain level until 1.8 seconds.

The existence of both positive and negative correlation coefficients as indicated by Figure 3.5 and Table 3.1 can be attributed to interindividual difference in shape of the ear canal. Diameter, length, and bending of the ear channel vary. The ear wearable sensor emits light toward the ear channel, and intensity of reflected light is converted into output voltage; intensity of reflected light is directly affected by bending and other shape parameters of the ear canal. Occlusal force (force applied to back teeth during eating) of adult men is estimated at 100 to 200 N [46].

Occlusal force considered in this study lies in the different range of 0 to 40 N. However, this does not discredit the measurement method described in this chapter because the measurement range can be expanded up to 200 N by modifying the occlusal force sensor.

As can be seen from Figure 3.6, output of the ear wearable sensor with respect to that of the occlusal force sensor varies at every measurement (low repeatability); however, correlation always remains positive. This can be explained by changes in relative positions of the sensor and ear canal, while movement of the ear is unchanged. That is, fixity of the ear wearable sensor should be improved.

Estimates obtained by weighted average and by least squares are closer to each other in Figure 3.7(a) than in Figure 3.7(b). This means that learning data (outputs of the ear wearable sensor and occlusal force sensor measured in the first through fourth runs) of subject A were more linear. The measured results of fifth run shown in Figure 3.7(a) are not linear, and therefore, are difficult to estimate from the learning data.

Results of estimating output of the occlusal force sensor from ear canal movement (Table 3.2 and Figure 3.7) suggest that with the proposed method, occlusal force can be estimated, at least in case that correlation coefficients between outputs of both sensors are predetermined for each subject. Requirement specifications for estimation of occlusal force have not been yet sufficiently explored. In future, we will conduct clinical tests to define adequate specifications including admissible errors, required resolution, etc.

The strong correlation between outputs of the occlusal force sensor and the ear wearable sensor can be utilized in a monitoring system for changes on occlusal force (magnitude of occlusal force in same measurement) estimated from values measured by the ear wearable sensor.

3.5 Conclusion

I am engaged in R&D on estimation of occlusal force from movement of the ear canal during occlusion using an ear wearable sensor (infrared LED and phototransistor). In this first report, I attached a wearable sensor to the right ear, and measured its output simultaneously to that of an occlusal force sensor clamped by the second molar teeth so as to examine relationship between occlusal force and movement of the ear canal. Thus, I obtained two findings. The first is the existence

of strong correlation between occlusal force and movement of the ear canal. However, output of the ear wearable sensor with respect to that of the occlusal force sensor varied in every measurement, though the correlation remained. The second is that with the proposed method, occlusal force can be estimated, at least in case that correlation coefficients between outputs of both sensors are predetermined for each subject.

In future, fixity of the ear wearable sensor should be improved to stabilize outputs of both sensors. In addition, an occlusal force sensor with measuring range up to 200 N must be developed. Further development is also needed regarding robust and accurate methods of data processing and estimation for the ear wearable sensor.

Chapter 4:
Simultaneous Measurement of Ear Canal Movement, Electromyography of the Masseter Muscle and Occlusal Force

4.1 Introduction

A patient who undergoes a gastrectomy operation for gastric cancer is at increased risk of nutritional disorders because of their reduced gastric function [17]. Recently, a study was conducted in Japan that used the number of chews during eating for adiposity risk evaluation. We have previously performed research and development of a reliable earphone-type chewing-count measuring device called the “earable RCC” [18]. The “earable” is a coined word connoting “wearable” and “ear”; “RCC” is an abbreviation of “reliable chewing-count measurement device”. The earable RCC is a device that measures the number of chews of the user wearing an earphone-type sensor (ear sensor) [5] performs; the total chewing count is displayed on a tablet terminal in real time. It can also record the number of chews and the measured waveform of chewing on the tablet. The earable RCC is used for experimental analysis of the dietary behavior of adipose patients and aids in providing meal instructions for post-gastrectomy patients in a medical institution in Japan.

In addition, we have studied occlusal force measurements as another application of the ear sensor, which has been used successfully in measuring mealtimes [40, 48, 49], respiratory rates [8], disturbances in breathing and posture during zazen [9], movements of the tongue [7], and the eyes and intentional blinking [6]. The next step is therefore to conduct studies regarding an estimation device of occlusal force based on the ear sensor. Previous occlusal force measurement systems required insertion of a pressure sensor into the patient’s mouth [50–61] or placement of electrodes on the patient’s jaw or cheek to measure the electromyography (EMG) for an occlusal force estimation [62–67].

In this research, the objective is to develop an occlusal force measurement device using the ear sensor from the earable RCC to measure the chewing count. Such a device would preclude using an intra-oral sensor or device during eating. And it does not require electrode pads, which can impede movement of the masticatory muscle and the jaw joint.

In Chapter 3, I conducted a study concerning the correlation between the occlusal force with light chewing on the second molar (occlusal force from approximately 0 to 40 N) and the movement of the ear canal measured using the ear sensor [47, 68]. With these results, the strong correlation between the occlusal force and ear canal movement was then investigated.

However, the maximum occlusal force measured on the second molar was approximately 500 N to 600 N for a healthy male subject and approximately 400 N for a male subject with dentures [69]. Therefore, I performed a similar experiment with the heavier chewing to confirm the correlation coefficient between the ear sensor output and the occlusal force over an appropriate force range.

This article presents results of the simultaneous measurement of the ear canal movement, the EMG of the masseter muscle, and the occlusal force (exceeding the maximum of 400 N), along with a discussion of each correlation based on the investigation of the Pearson product-moment correlation coefficient and the partial correlation coefficient. Section 4.2 describes the experimental system, the details of five subjects, the experimental method, the estimation method of the occlusal force, and the evaluation method for the estimation method. Sections 4.3–4.5 present the results, discussion, and conclusions, respectively.

4.2 Materials and Methods

4.2.1 Experimental System

In the experimental system (Figure 4.1), analog signals ranging from 0 V to 3.3 V are measured using the earphone-type sensor that we developed to measure ear canal movements (ear sensor). The signals of the GM-10 occlusal force meter (Nagano Keiki Co., Nagano, Japan) and the BR-1000 electromyograph (Nishizawa Electric Meters Manufacturing Co., Ltd., Nagano, Japan) are converted into digital signals using an analog-to-digital (AD) converter at a sampling frequency of 100 Hz with 12-bit resolution. These digital signals are then recorded with time-stamps on a storage device.

Figure 4.2 illustrates the measurement principle of the ear canal movement using the ear sensor. Occlusion is performed by the temporalis and masticatory muscles, including the masseter muscle and the temporomandibular joint. Occlusion causes a change in the shape of the ear canal near the masticatory muscles and the temporomandibular joint. During occlusion, the ear sensor measures the amount of the change in the ear canal shape optically and noninvasively.

A small photosensor (QRE1113, Fairchild Semiconductor International Inc., CA) is attached to the ear sensor. The photosensor houses a light-emitting diode (LED) with an emission wavelength of 940 nm and a phototransistor (Figure 4.1). The ear sensor irradiates the skin of the ear canal with infrared light; its reflected light is then received by the phototransistor to measure the change in the ear canal shape. In the ear sensor, the output increases as the amount of light reflected from the ear canal increases. Similarly, the output decreases as the amount of reflected light diminishes. The output offset voltage of the ear sensor is adjusted using the variable

resistor VR_1. The LED is provided along with a pulse wave generator to control light emissions. This pulse wave generator is synchronized with the AD convertor that is connected to the ear sensor. Because of the mechanisms involved, light is only emitted during AD conversion, and it is thus possible to enhance the LED emission (i.e., to increase the LED's forward current) in contrast to the always-emitting case. As a result of the large quantity of light produced, the effects of any ambient infrared light transmitted via the skin near the outer ear is suppressed and an improvement in the signal-to-noise (SN) ratio is expected. A processed medium-size commercial earplug, (EP3-BK-MPR, SureFire LLC., CA), is used as housing for the ear sensor.

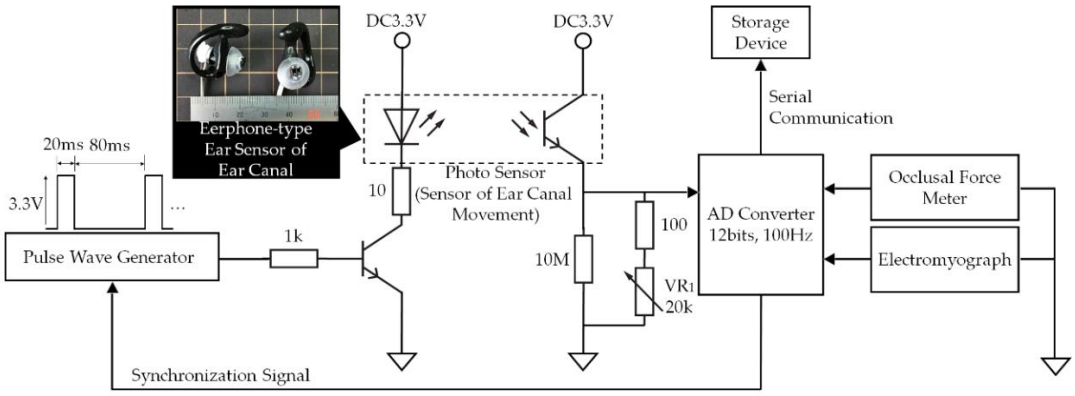

Figure 4.1. Experimental system. Analog signals ranging from 0 V to 3.3 V measured using the occlusal force meter, electromyography, and the ear sensor to measure the movement of the ear canal, are converted into digital signals by the analog-to-digital converter at a sampling frequency of 100 Hz with 12-bit resolution; the digital signals are then recorded together with time-stamps in a storage device.

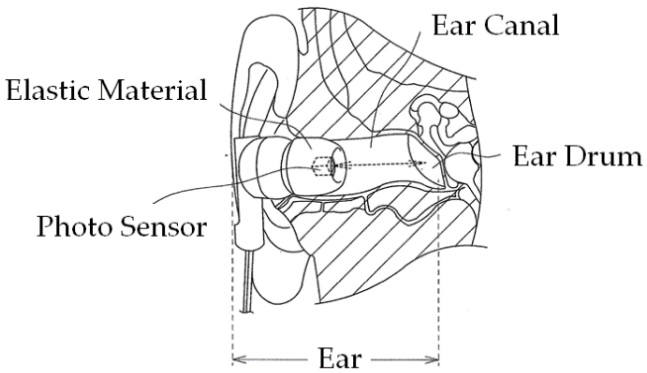

Figure 4.2. Measurement principle of ear canal movements using the ear sensor. Occlusion is performed by the temporalis and masticatory muscles, including the masseter muscle and the temporomandibular joint. Occlusion causes a change in the ear canal shape near the masticatory muscles and the temporomandibular joint. The ear sensor measures this change of shape during occlusion optically and noninvasively. A small photosensor is attached to the ear sensor. This photosensor houses a light-emitting diode (LED) with an emission wavelength of 940 nm and a phototransistor (Figure 4.1). The ear sensor irradiates the skin of the ear canal with infrared light, and the reflected light is then received by the phototransistor to measure the change in ear canal shape.

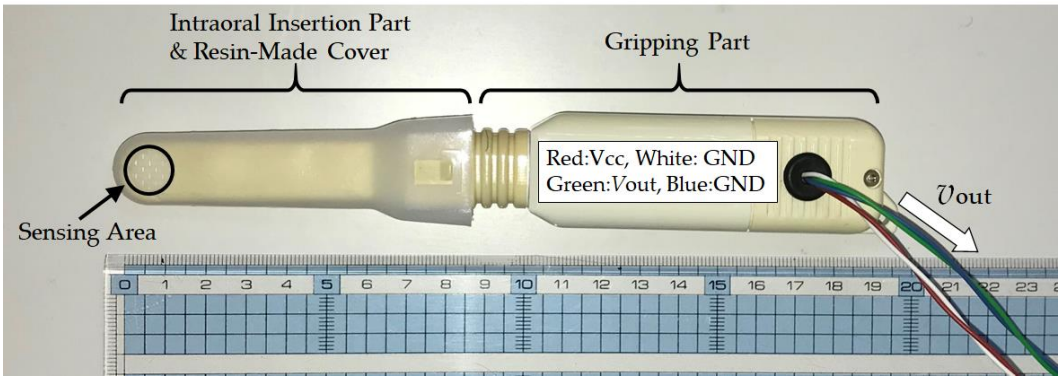

Figure 4.3. Photograph of the GM-10 occlusal force meter, which is constructed continuously of an intraoral insertion part and a gripping part; the intraoral insertion part (left side in figure) is 88 mm in length; the remaining 101 mm is the gripping part (right side). During measurements, the disposable resin-made cover is placed in advance on the intraoral insert. The subject then holds the gripping part in one hand and the sensor measures the occlusal force when the subject chews the tip (i.e., the sensing area) of the intraoral insertion part.

The GM-10 occlusal force meter is a small and lightweight occlusal force meter, with width, height, depth (i.e., total length) and mass of 29 mm, 18 mm, 189 mm, and 70 g, respectively (Figure 4.3). It is constructed continuously from an oral cavity insert of 88 mm (left side in Figure 4.3) and a gripping part (right side in Figure 4.3). During measurements, a disposable resin-made cover is placed on the intraoral insertion part in advance. The sensor measures the occlusal force that acts during chewing of the tip of the intraoral insertion part when the gripping part is held in one hand. The sensing area is located on the tip of the intraoral insertion part; propylene glycol liquid is sealed within its interior. The interior liquid pressure changes when the sensing area is chewed. The occlusal force meter then calculates the occlusal force from the liquid pressure, which is measured using a pressure sensor. The liquid pressure measurement and the occlusal force calculation are conducted using a signal processing circuit that is built into the gripping part. The calculated occlusal force is then displayed on a liquid crystal display device (back of the device in Figure 4.3) that is built into the gripping part. The signal processing circuit consists of a microprocessor, a memory circuit, a timer circuit, and a counter. This occlusal force meter was specially remodeled by its designers (coauthors Sakaguchi and Momose) for this research. Specifically, the remodeled force meter outputs a liquid pressure as an analog voltage v_{out} V, which ranges from 0 V to 3 V. In the experimental system (Figure 4.1), v_{out} is inputted by the AD convertor. The AD converted value is converted into an occlusal force F (in Newtons) using the equation,

$$F = 1985.6v_{\text{out}} - 75.07. \tag{4.1}$$

The BR-1000 electromyograph measures the surface EMG of the masseter muscle via the bipolar derivation method (Figure 4.4). This electromyograph consists of two detection electrodes, a ground electrode to determine the standard for the electric potential of the electromyograph, and a myogenic potential detection circuit.

Surface electrodes (bioload 45352V, GE Healthcare, Illinois, USA) was used. The EMG signal is bipolar and is led by the detection electrodes for input into the myogenic potential detection circuit consisting of a differential amplifier, a band-pass filter (BPF) with a passband of 100 Hz–1 kHz, an absolute value circuit, a low-pass filter with a cut-off frequency of 100 Hz, and a full-wave rectifier connected in cascade. This detection circuit outputs the envelope curve of a full-wave rectified signal in which the measured myogenic potential has been filtered and amplified. The electromyograph was also specially remodeled by its designers (coauthors Sakaguchi and Momose) for this research. Specifically, it outputs the envelope curve as an analog voltage v_{out} V with a range from 0 V to 3 V. In the experimental system (Figure 4.1), the analog value is inputted as an EMG value by the AD convertor.

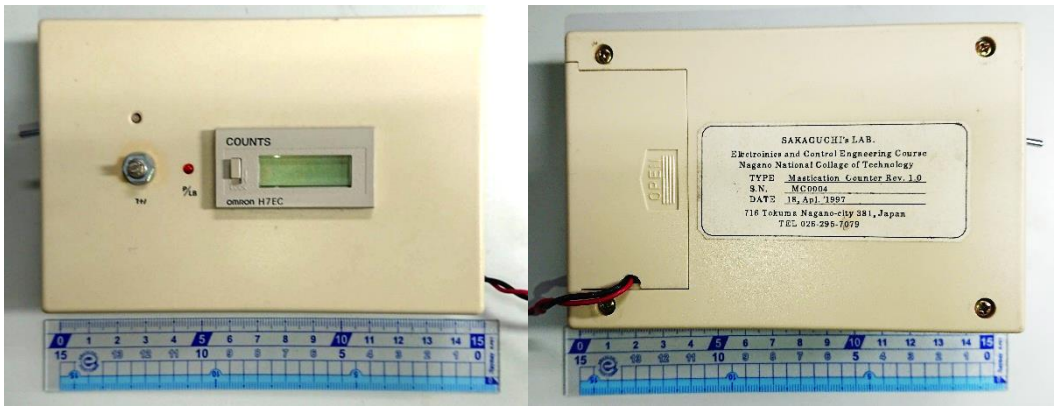

Figure 4.4. Photograph of the BR-1000 measures the surface EMG of the masseter muscle via the bipolar derivation method; the front (left side in figure) and the back (right side). The BR-1000 consists of two detection electrodes, a ground electrode to determine the standard for the electric potential of the electromyograph, and a myogenic potential detection circuit.

The AD convertor and the pulse wave generator (Figure 4.1) were implemented using a microprocessor (mbed LPC1768, Switch Science Inc., Tokyo,

Japan) and proprietary software (written in C++). The AD convertor inputs from 0 V to 3.3 V are converted into values ranging from 0.0000 to 1.0000, respectively.

A personal computer (PC; CF-SV78SJQP, Panasonic Corp., Japan; Windows 10 Pro Ver. 1803) was used as storage device. The microprocessor and the PC communicate via a CRS-232 specification interface running the communication software CoolTermWin Ver. 1.4.7 (freeware). The acquired data in the PC were processed using spreadsheet software (Microsoft Excel for Office 365, MOS 32-bit, Microsoft Corp., Washington, USA).

4.2.2 Subjects

The subjects were five young healthy people (males and females, aged 21 to 26, the average age being 23.2 years). They were assigned the labels A, B, C, D, and E. The subjects were able to chew the sensing area of the occlusal force meter thoroughly with their second molar teeth without difficulty and suffered no symptoms of pain or fatigue in the teeth and/or the jaw. People who were undergoing orthodontic treatment or being treated for a tooth or temporomandibular joint problem were excluded from the tests. In addition, subjects for whom the size of the ear sensor was a close fit to the size of their ear canal were selected. These people were free from symptoms of pain or fatigue in their ears. People undergoing treatment for ear problems were also excluded. In addition, any person who felt discomfort such as itching or for whom the seal-type electrode pad for the EMG measurements caused inflammation was excluded. The study was conducted in accordance with the Declaration of Helsinki, and received the approval of the “Ethics Review Procedures concerning research with human subjects at Shinshu University (Project

Identification Code: 227)"; after the context of the experiments was explained, each of the subjects signed a written consent.

4.2.3 Simultaneous Measurement of Ear Canal Movement, Masseter Muscle Electric Potential and Occlusal Force

Each of the five subjects performed six runs of the following experiment. The subject was seated in a chair with an ear sensor placed on their right ear to measure the movement of their ear canal; two surface electrodes for detection were placed on their right cheek (where the masseter muscle is located) to measure the EMG; a ground electrode was placed on their right clavicle. After placing the ear sensor and electrodes, the subject chewed the sensing area of the force meter thoroughly with their second molars. The subject begins with light chewing on the force sensor and gradually increases the pressure for approximately 2 s to a maximum pressure to hold the device in the mouth. Then, the pressure is relaxed to return to the initial conditions. The subject kept the head still during the experiment to prevent motion artifacts originating from the motion of the head during the measurements of the ear canal.

For hygiene reasons, the ear sensor was cleansed using a clean brush and disinfected using ethanol before and after each experiment. The subjects also cleaned their ear canal using a cotton swab before and after each experiment. The disposable cover of the occlusal force meter was replaced after each use and the body of the force meter was disinfected using ethanol after each use. In addition, the subjects gargled before and after each experiment. The disposable surface electrode of the EMG device was replaced for every subject. Before the electrodes were attached, the skin of the subject was wiped with ethanol as a skin preprocessing step.

4.2.4 Method of Occlusal Force Estimation from Ear Canal Movement Measured by Ear Sensor and Associated Evaluation Method

Among the six runs for each subject (Section 4.2.3), the output from both sensors in the five runs were used as a training set, and the remaining run was then used as a test set. The estimation accuracy was evaluated by K-fold cross-validation. For this study, the value of K is then six as six measurements were obtained. The precision of the k th run was calculated and used as a test set, whereas the other five runs were used as training sets. This was performed for k=1, 2, …, K.

In our previous research [47,70], a strong correlation was found with regard to the Pearson product-moment correlation coefficient between the ear sensor outputs and the occlusal force for weak occlusal forces of approximately 40 N; we then successfully obtained a regression line using the least squares method. Therefore, we also used single regression analysis to perform estimations. Specifically, the occlusal force estimated by single regression analysis was calculated by following procedures I to IV [corresponding to Equations (4.2) to (4.4) below]. The estimation accuracy was examined using the estimation evaluation index given in Equation (4.5). Additionally, an experiment with a strong occlusal force of more than 400 N was performed. We then discuss in Section 4.4 how enhancement of the occlusal force affects a specific correlation based on the experimental results.

I. Training set $\mathbf{T}_k = \{\mathbf{T}_{k1}, \mathbf{T}_{k2}, \mathbf{T}_{k3}, \mathbf{T}_{k4}, \mathbf{T}_{k5}\}$ is composed of the measured results from the five runs, with the exception of the k th measured result (test set). This was performed for k = 1, 2, …, 6. The i th element of the training set was composed of the occlusal force meter output f_{ij} (AD converted value) and the ear sensor output e_{ij} (AD converted value) measured within 2 s at a sampling frequency of 100 Hz, and was used as $\mathbf{T}_{ki} = \{ e_{ij}, f_{ij} | j = 1, 2, 3,\ldots,200\}$. j was the sequential number added to each data sample.

II. Second item SLOPE is a function used to obtain the single regression coefficient a_{ki} to estimate occlusal force from the ear sensor value, as shown in Equation (4.2). a_{ki} was determined for every element of the training set $\mathbf{T}_{ki}$:

$$a_{ki} = \mathrm{SLOPE}(\mathbf{T}_{ki}) = \frac{200\sum_{j=1}^{200} e_{ij}f_{ij} - \left(\sum_{j=1}^{200} e_{ij}\right)\left(\sum_{j=1}^{200} f_{ij}\right)}{200\sum_{j=1}^{200} e_{ij}^2 - \left(\sum_{j=1}^{200} e_{ij}\right)^2} \quad (4.2)$$

$k = 1, 2, 3, 4, 5, 6$

$i = 1, 2, 3, 4, 5$

III. The average $\overline{a_k}$ of the single regression coefficient a_{ki} obtained for every element of the training set $\mathbf{T}_{ki}$ was determined using Equation (4.3):

$$\overline{a_k} = \frac{1}{5}\sum_{i=1}^{5} a_{ki} \quad (4.3)$$

$k = 1, 2, 3, 4, 5, 6$

IV. Let f_{k0} be the initial value of the occlusal force in the k th test, and e_{k0} be the initial value from the ear sensor in the k th test. The estimated value $\tilde{f}_{kj}$ was determined by substitution of the measured value from the ear sensor e_{kj} into Equation (4.4):

$$\tilde{f}_{kj} = \bar{a}_k\left(e_{kj} - e_{k0}\right) + f_{k0} \quad (4.4)$$

$k = 1, 2, 3, 4, 5, 6$

$j = 1, 2, 3, \ldots, 200$

The precision evaluation index $NRMSE_k$ given in Equation (4.5) was used to evaluate the accuracy of the estimated value $\tilde{f}_{kj}$:

$$NRMSE_k = \frac{RMSE_k}{\tilde{f}_{k\mathrm{MAX}} - \tilde{f}_{k\mathrm{MIN}}} \quad (4.5)$$

$k = 1, 2, 3, 4, 5, 6$

The root-mean-square error $RMSE_k$ was determined using Equation (4.6), where $\tilde{f}_{k\mathrm{MAX}}$ and $\tilde{f}_{k\mathrm{MIN}}$ respectively indicate the maximum and minimum estimated values in $\tilde{f}_{k1}$, $\tilde{f}_{k2}$, $\tilde{f}_{k3}$,..., $\tilde{f}_{k200}$:

$$RMSE_k = \sqrt{\frac{1}{200}\sum_{j=1}^{200}\left(f_{kj} - \tilde{f}_{kj}\right)^2} \tag{4.6}$$

$k = 1, 2, 3, 4, 5, 6$

4.3 Results

4.3.1 Simultaneous Measurement Results for Ear Canal Movement, Masseter Muscle and Occlusal Force for Earphone-Type Occlusal Force Sensor

Listed in Table 4.1 are the average and square-root values of the unbiased variance from the Pearson product-moment correlation coefficient between the ear sensor value and the occlusal force, the ear sensor value and the EMG value, and the EMG value and the occlusal force obtained in the six runs for all six subjects. The square root of the unbiased variance was used to show the dispersion of the average in the correlation coefficients. When the variation of the average in such a coefficient decreases, the value of the square root of the unbiased variance also decreases. Based on the results (Table 4.1), Table 4.2 lists the average and square-root values of the unbiased variance of the partial correlation coefficient in the six runs when eliminating the effect of the EMG value from the correlation coefficient between the ear sensor value and the occlusal force. A similar listing (Table 4.2) is given for the effect of the ear sensor value from the correlation coefficient between the EMG value

and the occlusal force. When estimating the occlusal force with the ear sensor value (Section 4.2.4), the absolute value of the average of the correlation coefficient and the partial correlation coefficient should be close to 1, whereas the square root of the unbiased variance should be close to 0.

Table 4.1. Results for the coefficients of correlation. Average and square-root values are given of the unbiased variance from the coefficients of correlations between ear sensor value and occlusal force, ear sensor value and electromyography (EMG) value, and the EMG value and occlusal force, obtained over six runs for subjects A through E using the experimental method of Section 4.2.4.

Subject	Ear Sensor—Occlusal Force		Ear Sensor—EMG		EMG—Occlusal Force	
	Average	Square Root of Unbiased Variance	Average	Square Root of Unbiased Variance	Average	Square Root of Unbiased Variance
A	−0.994	0.004	−0.980	0.005	0.983	0.006
B	−0.951	0.026	−0.925	0.032	0.983	0.006
C	0.990	0.004	0.979	0.012	0.979	0.013
D	−0.960	0.025	−0.908	0.036	0.955	0.020
E	0.981	0.007	0.958	0.026	0.963	0.038

From Table 4.1, the correlation coefficient between the ear sensor value and the occlusal force and the correlation coefficient between the ear sensor value and the EMG value were negative for subjects A, B and D, but were positive for subjects C and E. The correlation coefficient between the EMG value and the occlusal force was positive for all subjects. The correlation coefficient can be a positive correlation or a negative correlation depending on the specific subject. In addition, the subjects who showed positive (negative) correlations only showed positive (negative) correlations in all six runs. The absolute average of the correlation coefficient

between the ear sensor and the occlusal force for all subjects was more than 0.951 and the square root of the unbiased variance was 0.026 or less. The absolute average of the correlation coefficient between the ear sensor value and the EMG value for all subjects was more than 0.908, whereas the square root of the unbiased variance was 0.036 or less. In addition, the absolute average of the correlation coefficient between the EMG value and the occlusal force for all subjects was more than 0.955, whereas the square root of the unbiased variance was 0.038 or less.

Subject B showed the highest absolute average for the correlation coefficient between the EMG value and the occlusal force; the average was 0.983, the square root of the unbiased variance was 0.006. The minimum absolute correlation coefficient in the six runs was 0.974 and the maximum was 0.990. Subject D showed the lowest absolute average for the correlation coefficient between the ear sensor value and the occlusal force; the average was 0.955, the square root of the unbiased variance was 0.020. The minimum absolute correlation coefficient in the six runs was 0.929 and the maximum was 0.979.

From Table 4.2, the partial correlation coefficient between the ear sensor value and the occlusal force and the partial correlation coefficient between the ear sensor value and the EMG value were negative for subjects A, B and D, but were positive for subjects C and E. The partial correlation coefficient between the EMG value and the occlusal force was positive for all subjects. The relationships for the dependence on negative or positive values of the partial correlation coefficient for the specific subjects were the same as those for the correlation coefficient. The partial correlation coefficients between the ear sensor value and the occlusal force were higher than the partial correlation coefficients between the EMG value and the occlusal force for all subjects.

Table 4.2. Results for partial correlation coefficients. Based on the results given in Table 4.1, the average and square root values of the unbiased variance of the partial correlation coefficient over six runs while eliminating the effect of the EMG value from the correlation coefficient between the ear sensor value and the occlusal force are given; the average and square root of the unbiased variance of the partial correlation coefficient over six runs while eliminating the effect of the ear sensor value from the correlation coefficient between the EMG value and the occlusal force are also given.

Subject	Ear Sensor—Occlusal Force		EMG—Occlusal Force	
	Average	Square Root of Unbiased Variance	Average	Square Root of Unbiased Variance
A	−0.829	0.153	0.350	0.286
B	−0.616	0.186	0.855	0.103
C	0.728	0.132	0.367	0.277
D	−0.7578	0.169	0.639	0.302
E	0.628	0.329	0.482	0.485

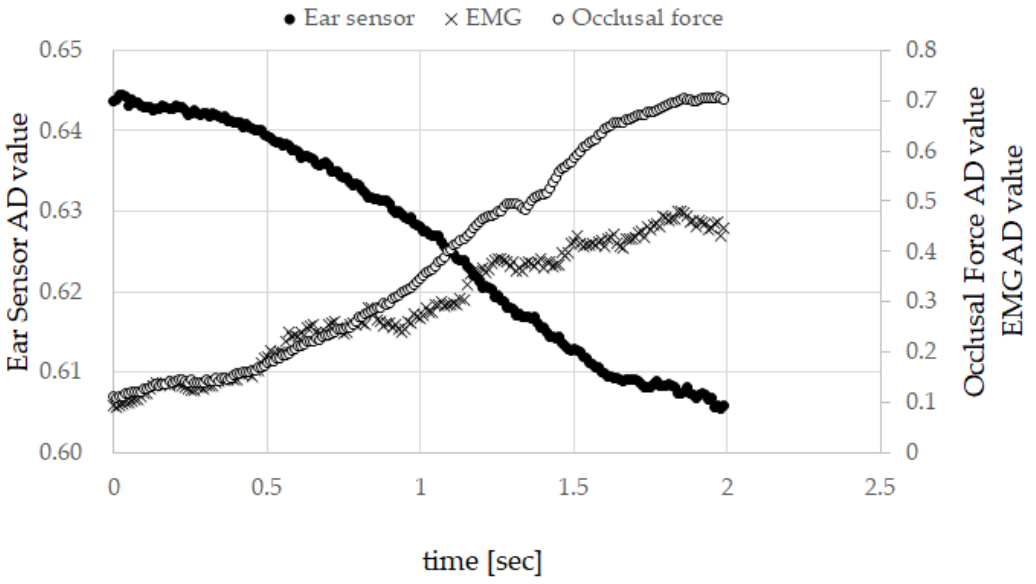

Figure 4.5. Measured results for subject A. The graph shows the measured results for which the correlation coefficient between the ear sensor value and the occlusal force was the highest among the six runs of subject A.

The measured results for subject A (Figure 4.5) show the correlation coefficient between the ear sensor value and the occlusal force was the highest in the six runs. This measured value also showed the highest correlation between the ear

sensor value and the EMG value. Here, the horizontal axis represents time, the left vertical axis represents the ear sensor value (i.e., the AD converted value), and the right vertical axis represents the EMG value (the AD converted value) and the occlusal force (the AD converted value). From Tables 4.1 and 4.2, subject A had the highest absolute average for the correlation coefficient between the ear sensor value and the occlusal force among all subjects; the highest absolute average for the correlation coefficient between the ear sensor value and the EMG value among all subjects; the second highest average for the correlation coefficient after subject B; the highest absolute average for the partial correlation coefficient between the ear sensor value and the occlusal force in all subjects; and the lowest average for the correlation coefficient between the EMG and the occlusal force among all subjects. Figure 4.5 also provides an overview of these characteristics.

4.3.2 Results for Estimation of Occlusal Force from Ear Canal Movement (Ear Sensor Value)

The average $\bar{a}$ from $\overline{a_k}$ (k = 1, 2, …, 6) as determined using Equation (4.3) and the square root of the unbiased variance for each subject are listed in Table 4.3. Subject A shows the lowest square root of the unbiased variance for all subjects, with a value of 1.749. The measurement results for the ear sensor and the occlusal force in runs 1–6 for subject A are plotted in Figure 4.6. Here, the horizontal axis represents the ear sensor-measured value, while the vertical axis represents the measured occlusal force value. The trends in the six runs are all similar inclinations with small differences in the offset values of the ear sensor values. Figure 4.6 shows that the square root of the unbiased variance for subject A may be small, as indicated in Table 4.3. Subject B shows the highest square root of the unbiased variance among

all subjects, with a value of 11.018. The dispersion of $\overline{a_k}$ for subject B was greater than that for the other subjects.

Table 4.4 shows the results of cross-validation with regard to the estimated occlusal force from the ear sensor value Equation (4.4) using the method described in Section 4.2.4. Specifically, the $RMSE_k$ values for subjects A through E determined using Equation (4.6), the maximum estimated value $\tilde{f}_{k\mathrm{MAX}}$, the minimum estimated value $\tilde{f}_{k\mathrm{MIN}}$ the difference between $\tilde{f}_{k\mathrm{MAX}}$ and $\tilde{f}_{k\mathrm{MIN}}$ (estimated width) and the average of the cross-validation results over six runs for the calculated results for the precision evaluation index $NRMSE_k$, Equation (4.5), are shown. Higher values for the estimated width in Table 4.4 represent wider estimation ranges. A lower $RMSE_k$ represents higher estimation accuracy for the same estimated width. Because the estimated width differed depending on the specific subject, a precision evaluation index $NRMSE_k$ in which the effect of the estimated width was eliminated was used for the evaluation. A lower $NRMSE_k$ value corresponds to higher evaluation accuracy. Subject A showed the highest accuracy (i.e., the lowest value of $\overline{NRMSE}$), with $\overline{RMSE}$ of 0.034, an estimated width ($\overline{\tilde{f}_{\mathrm{MAX}} - \tilde{f}_{\mathrm{MIN}}}$) of 0.539, and an $\overline{NRMSE}$ value of 0.066. The estimated values for subject A were translated into occlusal forces using Equation (4.1) and gave values for $\overline{\tilde{f}_{\mathrm{MAX}}}$ of 1117 N and $\overline{\tilde{f}_{\mathrm{MIN}}}$ of 47 N. Subject B showed the highest value for $\overline{NRMSE}$, with $\overline{RMSE}$ of 0.097, an estimated width of 0.396, and an $\overline{NRMSE}$ value of 0.287. The estimated values for subject B were translated into occlusal forces using Equation (4.1) and gave values for $\overline{\tilde{f}_{\mathrm{MAX}}}$ of 801 N and $\overline{\tilde{f}_{\mathrm{MIN}}}$ of 14 N.

Subject A showed the largest estimated width and subject C showed the smallest estimated width, where the latter is 0.204.

Table 4.3. Average estimation results for the single regression coefficient and the square-root of the unbiased variance. The average $\bar{a}$ from $\overline{a_k}$ (k = 1, 2,…, 6) determined using Equation (4.3) and the square-root of the unbiased variance of $\overline{a_k}$ for each subject are given.

Subject	$\bar{a}$	Square Root of Unbiased Variance
A	−16.106	1.749
B	−22.856	11.018
C	12.003	5.024
D	−8.963	3.772
E	18.754	5.262

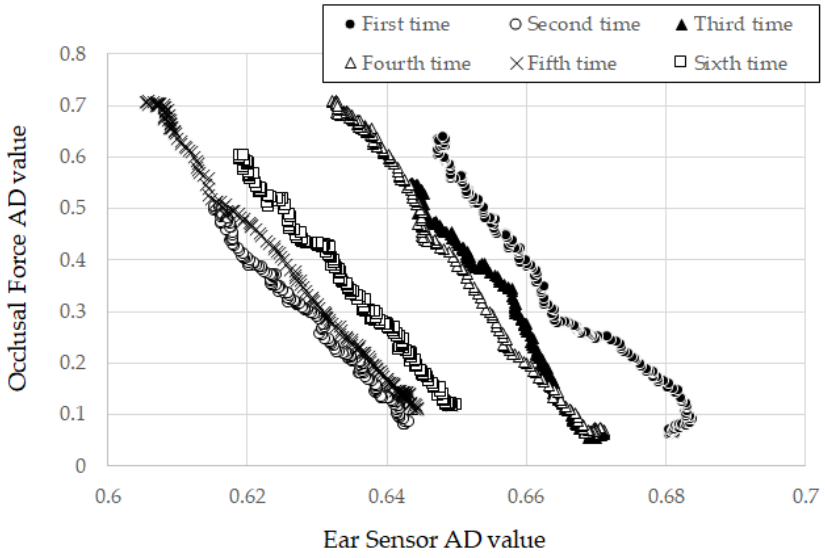

Figure 4.6. Measurement results for ear sensor and occlusal force over the first through sixth runs for subject A. Here, the horizontal axis represents the ear sensor-measured value, while the vertical axis represents the measured occlusal force value.

Table 4.4. Average precision error and maximum and minimum for each subject. Here, the precision errors $RMSE_k$ of subjects A through E determined using Equation (4.6) are shown, along with the maximum estimated value $\tilde{f}_{k\mathrm{MAX}}$, the minimum estimated value $\tilde{f}_{k\mathrm{MIN}}$, the difference between $\tilde{f}_{k\mathrm{MAX}}$ and $\tilde{f}_{k\mathrm{MIN}}$ (i.e., the estimated width), and the average of the cross-validation results over six runs for the calculated results for the precision evaluation index $NRMSE_k$ defined in Equation (4.5).

Subject	$\overline{RMSE}$	$\overline{\tilde{f}_{\mathrm{MAX}}}$	$\overline{\tilde{f}_{\mathrm{MIN}}}$	$\overline{\tilde{f}_{\mathrm{MAX}} - \tilde{f}_{\mathrm{MIN}}}$	$\overline{NRMSE}$
A	0.034	0.600	0.061	0.539	0.066
B	0.097	0.441	0.045	0.396	0.287
C	0.049	0.258	0.054	0.204	0.267
D	0.048	0.270	0.054	0.216	0.238
E	0.092	0.447	0.018	0.429	0.208

4.4 Discussion

In related studies concerning the estimation of the occlusal force, one active area of investigation involves using EMG. In research on the correlation between the EMG and the occlusal force relevant to this study, a value for the correlation coefficient of 0.75 was given in [64] and 0.626 in [66]. The measurement device that I used for EMG gave 0.955 or more for the correlation coefficient between the EMG and the occlusal force. These values of the correlation coefficient from these devices are not comparable because they have differences in structure and data processing techniques. Nevertheless, a correlation between the EMG and the occlusal force has been performed with the three devices and therefore I believe comparing my EMG measurement results as well as the measurement results of the ear sensor offers a means to contrast related research indirectly.

In Chapter 3, a strong correlation between the ear sensor outputs and the occlusal force for weak occlusal forces of approximately 40 N had been investigated. In this chapter, I performed experiments with strong occlusal forces exceeding 400 N. Therefore, as shown in Table 4.1, each absolute average of the correlation coefficient between the ear sensor value and the occlusal force, the correlation coefficient between the ear sensor value and the EMG value, and the correlation coefficient between the EMG value and the occlusal force showed high correlation for all subjects. Additionally, the dispersion of the correlation coefficient was low, as indicated by the fact that the square root of the unbiased variance was low. Although the number of subjects was small, these considerations are roughly possible because the five subjects, whose ages and sex were different, performed the measurement results in a consistent manner. However, in order to obtain statistically significant results, it is essential to increase the number of subjects, and in the future, I will increase the number of subjects of various types.

The reason for the existence of both positive and negative correlation coefficients (Table 4.1) can be attributed to inter-individual differences in ear canal shape. The diameter, length and bending of the ear canal can all vary. Because the ear sensor emits light toward the ear canal and outputs a voltage converted from the intensity of the reflected light, inter-individual differences such as bending of the ear canal affect the intensity of the reflected light directly. The partial correlation coefficient exceeded 0.616 for all subjects, indicating that there is a correlation (Table 4.2). In Table 4.1, the correlation coefficient between the ear sensor and the occlusal force was as high as the correlation coefficient between the EMG and the occlusal force. Moreover, the results for the correlation coefficient between the ear sensor and the occlusal force (Table 4.2) was established independently of EMG. Using the correlation coefficient and the partial correlation coefficient, the correlation between

the ear sensor value and the occlusal force can be investigated; this represents an adequate method to acquire the estimated occlusal force from the value measured by the ear sensor via single regression analysis. Additionally, the low *RMSE* and *NRMSE* values from the experimental results also supported the appropriateness of the method. To improve the estimation accuracy, both collecting the measurement values of the ear canal movement from a subject of various characteristics by increasing the number of subjects and increasing the amount of learning data (i.e., for the training set) for the estimation process are valid approaches. However, the additive average value of a_{ki} is used for the $\overline{a_k}$ value at present. To achieve improved estimation accuracy, I must consider other methods such as acquisition of a median and a mode from a histogram formed with increased quantities of learning data. Additionally, I will improve the estimation method and develop a data processing technique for the ear sensor with fewer errors and high robustness.

In this experiment, the value of the ear sensor changed proportionally with increasing occlusal force and had not attained a state of saturation for all subjects (Figure 4.6). However, I speculate that the ear sensor value attains a state of saturation for an occlusal force outside the range applied in the experiment. In such instances, ear canal movements may be hindered by an anatomical factor of the muscle and the internal skeleton.

This study was conducted with the supposition that the ear sensor does not misread a measurement. From the square root of the unbiased variance (Table 4.3) and the value of $\overline{NRMSE}$ in Equation (4.4), this supposition appears to hold in the range of the measurement results, because there was no measurement error troubling the estimation method indicated in Equation (4.4). However, there is concern that, with the movement of the head, a motion artifact may prompt mistakes in measurement. Because commercial earplugs were used to house the ear sensor. The

earplugs do not fit perfectly for each subject. Therefore, the sensor may shake from movement of the subject's head, and the shaking may affect measurement values. Mitigation of these concerns is an open problem for the future, as is perfect earplug fitting for each subject, which may help to eliminate motion artifact from measurement results.

Finally, I describe a future scenario for developing an occlusal force estimation system (referred to as "earable Ω") with the estimation method in Section 4.2.4 (estimation method using the measured value from ear sensor). The "OMEGA" of the name "earable Ω" is an abbreviation of "Occlusal Measurement and its Estimation system, General Availability version". The earable Ω comprising a measurement start button, a calibration button, and a small liquid crystal display device, is an ear phone shaped device including ear sensor. The earable Ω is put on the ear on the same side of the teeth used for measurement. The measured values from the ear sensor are recorded in memory with the digital signals converted by the AD converter at a sampling frequency of 100 Hz and resolution of 12 bit. Not only are measured results recorded but also $\overline{a_k}$, both of which are needed in advanced to estimate the occlusal force using the estimation method in Section 4.2.4. Only the maximum occlusal force on the loading small liquid crystal needs to be displayed by the earable Ω device. A display of its time-series variation can be had by sending the data to an external device such as a smart phone, from which the data can be further processes.

To obtain a training set to establish $\overline{a_k}$, gummy candy, which has a known hardness (adjusted hardness) is to be used instead of the occlusal force meter as in this study. Once the calibration button is activated, then the gummy candy is chewed with the teeth used for the measurement. The measured result of the first "single bite"

is used for the training set. Repeated chewing of several gummy candies increases the data needed for $\overline{a_k}$ and improves the estimation accuracy.

When performing occlusal force estimations, the user places the earable Ω on the ear and brings the top back tooth and the bottom back tooth into contact without chewing (the occlusal force is then 0 N). The user next activates the start button of the earable Ω and chews. For the two-second duration from activation, measurements are recorded in memory. The occlusal force is then estimated using Equation (4.4) based on these measurements. The measured value from the ear sensor on activation is used as the initial value for e_{k0} with f_{k0} set to 0.

As a next step, I shall verify the idea by making a prototype of the earable Ω. The required specification necessary to estimate the occlusal force is still being studied along with other research organizations. In future, clinical experiments need to be undertaken to help determine suitable specifications regarding resolution and tolerance of the device.

4.5 Conclusion

I am engaged in research and development of a method for occlusal force estimation based on the movement of the ear canal and a device that uses the proposed method. The occlusal force can be measured during eating if it is possible to estimate the occlusal force from the movement of the ear canal. The method does not use electrode pads, which impede the movement of the masticatory muscle and the jaw joint. An earphone that I originally researched and developed was used to measure the ear canal movement. The ear sensor has the same shape as an internal-type earphone and contains an infrared LED and a phototransistor. The LED irradiates the inside of ear canal with light and the reflected light is received by the

phototransistor to measure the change in the ear canal shape. In the ear sensor, the output increases in tandem with the amount of light reflected from the ear canal. Similarly, the output decreases in tandem with the amount of light reflected from the ear canal. The output offset voltage of the ear sensor can be adjusted using the variable resistor VR_1. In this work, I simultaneously measured the movement of the ear canal, the surface electromyography (EMG) of the masseter muscle and the occlusal force six times each for five subjects as a basic study for the development of an occlusal force meter. I used these results to investigate the Pearson product-moment correlation coefficient between the ear sensor value and the occlusal force, and the partial correlation coefficient between the ear sensor values and the occlusal force when eliminating an effect of the EMG. Additionally, I investigated the average of the partial correlation coefficient over the six runs and the absolute value of the average for each subject. The results for the absolute value were indicative of strong correlation, with the correlation coefficients exceeding 0.951 for all subjects. The lowest partial correlation coefficient shown by any subject was 0.616, while the highest partial correlation coefficient shown by any subject was 0.829. These values were also indicative of correlation. I then estimated the occlusal force via single regression analysis using the data from the six runs for each of the subjects. There is a correlation between the ear sensor value and the occlusal force that can be investigated that provides an adequate method to estimate the occlusal force from the ear sensor value via single regression analysis. The results of evaluation of the proposed method using the cross-validation method indicated that the root-mean-square error ($RMSE_k$) obtained from comparison of the actual value with the estimates for the five subjects ranged from 0.034 to 0.097.

In future work, I intend to realize an occlusal force estimation device through improvement of the estimation accuracy by increasing the numbers of

learning data, development of a data processing technique with fewer errors and high robustness that is suitable for use with the ear sensor, and improvement of the estimation method.

Chapter 5:

Conclusions

In chapter 2, I described a method for estimating meal times based on temporal changes in the amount of light received by a small optical sensor composed of an LED and a phototransistor inserted in the right ear canal. The device shines light toward the inner ear canal and receives light reflected back by the ear canal. An experiment performed using seven subjects was successful in estimating meal times in all subjects within a set range of error. Furthermore, an analysis of the measured values during running and chewing obtained from the same sensor inserted into the left and right ear canals of four subjects revealed that measurements from the left and right ear canals were strongly correlated during running, but not correlated during chewing. These findings allow running and chewing to be differentiated based on correlation coefficients.

Through Chapters 3 to 4, I am engaged in research and development of a method for occlusal force estimation based on the movement of the ear canal and a device that uses the proposed method. The occlusal force can be measured during eating if it is possible to estimate the occlusal force from the movement of the ear canal. The method does not use electrode pads, which impede the movement of the masticatory muscle and the jaw joint. The ear sensor that I originally researched and developed in Chapter 2 was also used to measure the ear canal movement.

In Chapter 3, I conducted an experiment involving six subjects about the correlation between the occlusal force with light chewing on second molar (occlusal force from approximately 0 to 40 N) and the movement of the ear canal measured using the ear sensor. Using the results, the strong correlation between the occlusal force and the movement of the ear canal was then investigated. However, the maximum occlusal force measured on the second molar was approximately 500 N to 600 N for healthy male subjects and approximately 400 N for a male subject with dentures. Therefore, I performed a similar experiment with heavy chewing to confirm

the correlation coefficient between the occlusal force and the ear sensor output over an appropriate occlusal force range.

In Chapter 4, I simultaneously measured the movement of the ear canal, the surface electromyography (EMG) of the masseter muscle and the occlusal force six times each for five subjects as a basic study for the development of an occlusal force meter. I used these results to investigate the Pearson product-moment correlation coefficient between the ear sensor value and the occlusal force, and the partial correlation coefficient between the ear sensor values and the occlusal force when eliminating an effect of the EMG. Additionally, I investigated the average of the partial correlation coefficient over the six runs and the absolute value of the average for each subject. The results for the absolute value were indicative of strong correlation, with the correlation coefficients exceeding 0.951 for all subjects. The lowest partial correlation coefficient shown by any subject was 0.616, while the highest partial correlation coefficient shown by any subject was 0.829. These values were also indicative of correlation. I then estimated the occlusal force via single regression analysis using the data from the six runs for each of the subjects. There is a correlation between the ear sensor value and the occlusal force that can be investigated that provides an adequate method to estimate the occlusal force from the ear sensor value via single regression analysis. The results of evaluation of the proposed method using the cross-validation method indicated that the root-mean-square error ($RMSE_k$) obtained from comparison of the actual value with the estimates for the five subjects ranged from 0.034 to 0.097.

In future, the proposed mealtime estimation technique can be updated by developing a method for estimating the amount of movement of the body by analyzing waveforms during running. In addition to improving my meal time estimation algorithm and continuing to investigate methods for differentiating

running and chewing, I aim to conduct further experiments using larger subject samples. In addition, I intend to realize an occlusal force estimation device through improvement of the estimation accuracy by increasing the numbers of learning data, development of a data processing technique with fewer errors and high robustness that is suitable for use with the ear sensor, and improvement of the estimation method.

The devices and measurement techniques proposed in this thesis can contribute to the improvement of people life quality. By objectively using numerical value, they review the user's status such as their domestic dietary habits, exercise quantity and body weight and purpose them for self-health maintenance.

Chapter 6:

References

1. Pantelopoulos, A.; Bourbakis, NG.; A Survey on Wearable Sensor-Based Systems for Health Monitoring and Prognosis, *IEEE Transactions on Systems Man and Cybernetics Part C (Applications and Reviews)*, 40 (1), February 2010.

2. Piwek, L.; Ellis, DA.; Andrews, S.; Joinson, A. The Rise of Consumer Health Wearables: Promises and Barriers, *PLoS Med*. 2016, 13 (2), 9 pages. DOI:10.1371/journal.pmed.1001953.

3. Lukowixs, P.; Lyons, K.; ISWC 09: 13th International Symposium on Wearable Computers, *IEEE Pervasive Computing* 2010, 9 (2), pp. 6-7.

4. NTT. "hitoe". http://www.docomo.biz/html/product/hitoe/

5. Taniguchi, K.; Nishikawa, A.; Miyazaki, F.; Kokubo, A. Input Device, Wearable Computer, and Input Method. U.S. Patent No. US8994647, 31 March 2015.

6. Taniguchi, K.; Horise, Y.; Nishikawa, A.; Iwaki, S. A novel wearable input device using movement of ear-canals. In Proceedings of the Textile Bioengineering and Informatics Symposium 2012 (TBIS2012), Ueda, Japan, 9–11 August 2012.

7. Taniguchi, K.; Kondo, H.; Kurosawa, M.; Nishikawa, A. Earable TEMPO: A novel, hands-free input device that uses the movement of the tongue measured with a wearable ear sensor. *Sensors* 2018, 18, 733.

8. Taniguchi, K.; Nishikawa, A. Earable POCER: Development of a point of care ear sensor for respiratory rate measurement. *Sensors* 2018, 18, 2273–2291.

9. Taniguchi, K.; Nishikawa, A. Earable ZEN: Development of an earphone-type zazen support wearable system. *J. Healthc. Eng.* 2018, 2018, 1838563.

10. Mochizuki Y, Shirakawa K, Abe K, Tokinobu H, Masumi M. The relationship about risk factors of Arteriosclerosis and the habit of diet. *J. Ningen Dock* 1998, 13, pp.13-17 (in Japanese)

11. Nakamori T, Obata K, Kakuta Y, Tsushima M. Effects of fast eating habits on the body. *J. Japan Mibyou System Association* 2015, 11 (1), pp.73-76. (in Japanese)

12. Iimura T, Arai Y, Fukumoto M, Takayama M, Abe Y, Asakura K, Nishiwaki Y, Takebayashi T, Iwase T, Komiyama K, Gionhaku N, Hirose N. Maximum Occlusal Force and Physical Performance in the Oldest Old: The Tokyo Oldest Old Survey on Total Health. *J Am Geriatr Soc.* 2012, 60 (1), pp. 68-76.

13. Yatani H, Akagawa Y. Do Occlusion and Masticatory Function Contribute to General Health and Longevity?. *Ann Jpn Prosthodont Soc* 2012, 4, pp. 372-374. (in Japanese)

14. Hatori, M.; Vollmers, C.; Zarrinpar, A.; DiTacchio, L.; Bushong, E.A.; Gill, S.; Leblanc, M.; Chaix, A.; Joens, M.; Fitzpatrick, J.A.J.; et al. Time-Restricted Feeding without Reducing Caloric Intake Prevents Metabolic Diseases in Mice Fed a High-Fat Diet. *Cell Metab.* **2012**, *15*, 848–860.

15. Nasu I, Saito Y. Active life expectancy for elderly Japanese by chewing ability. *Jpn J Public Health.* 2005;53:411–423. (in Japanese)

16. Lotte Rhythmi-Kamu Webpage: https://kamukoto.jp/rhythmi-kamu/. (in Japanese). Accessed September 11, 2017.

17. Eagon JC, Miedema BW, Kelly KA. Postgastrectomy syndromes. *Surg Clin North Am.* 1992;72:445–465.

18. Taniguchi K, Kondo H, Tanaka T, Nishikawa A. Earable RCC: development of an earphone-type reliable chewing-count measurement device. *J Healthc Eng*. 2018;2018:8. Article ID 6161525

19. Winokur, E.S.; He, D.D.; Sodini, C.G. A wearable vital signs monitor at the ear for continuous heart rate and Pulse Transit Time measurements. In Proceedings of the 2012 Annual International Conference of the IEEE Engineering in Medicine and Biology Society (EMBC), San Diego, CA, USA, 28 August–1 September 2012; pp. 2724–2727.

20. Shen, C.L.; Kao, T.; Huang, C.T.; Lee, J.H. Wearable band using a fabric–based sensor for exercise ECG monitoring. In Proceedings of the 2006 10th IEEE International Symposium on Wearable Computers, Montreux, Switzerland, 11–14 October 2006; pp. 143–144.

21. Hung, K.; Zhang, Y.T.; Tai, B. Wearable Medical Devices for Tele-Home Healthcare. In Proceedings of the *26th Annual International Conference of the IEEE on Engineering* in *Medicine* and *Biology Society,* San Francisco, CA, USA, 1–4 September 2004; pp. 5384–5387.

22. Wei, J. How Wearables Intersect with the Cloud and the Internet of Things Considerations for the Developers of Wearables. *IEEE Consum. Electron. Mag.* **2014**, *3*, 53–56.

23. Constant, N.; Prawl, O.D.; Johnson, S.; Mankodiya, K. Pulse-glasses: An unobtrusive, wearable HR monitor with Internet-of-Things functionality. In Proceedings of the 2015 IEEE 12th International Conference on Wearable and Implantable Body Sensor Networks (BSN), Cambridge, MA, USA, 9–12 June 2015; pp. 1–5.

24. Salehizadeh, S.M.A.; Noh, Y.; Chon, K.H. Heart rate monitoring during intense physical activities using a motion artifact corrupted signal reconstruction algorithm in wearable electrocardiogram sensor. In Proceedings of the IEEE 1st International Conference on Connected Health: Applications, Systems and Engineering Technologies (CHASE), Washington, DC, USA, 27–29 June 2016; pp.157–162.

25. Thomas, S.S.; Nathan, V.; Zong, C.; Soundarapandian, K.; Shi, X.; Jafari, R. BioWatch: A Noninvasive Wrist-Based Blood Pressure Monitor That Incorporates Training Techniques for Posture and Subject Variability. *IEEE J. Biomed. Health Inform.* **2016**, *20*, 1291–1300.

26. Zhang, H.; Sun, Y.; Lu, Y.; Lan, J.; Ji, Y. A novel motion and Noise Artifacts Reduction Mechanism (MNARM) for wearable PPG-based heart rate extraction. In Proceedings of the 2015 IET International Conference on Biomedical Image and Signal Processing (ICBISP 2015), Beijing, China, 19 November 2015; pp. 1–4.

27. Preejith, S.P.; Alex, A.; Joseph, J.; Sivaprakasam, M. Design, development and clinical validation of a wrist-based optical heart rate monitor. In Proceedings of the 2016 IEEE International Symposium on Medical Measurements and Applications (MeMeA), Benevento, Italy, 15–18 May 2016; pp. 1–6.

28. Ye, X.; Chen, G.; Cao, Y. Automatic eating detection using head-mount and wrist-worn accelerometers. In Proceedings of the 17th International Conference on e-Health Networking, Application & Services (HealthCom), Boston, MA, USA, 14–17 October 2015; pp. 578–581.

29. Long, X.; Yin, B.; Aarts, R. Single-accelerometer-based daily physical activity classification. In Proceedings of the Annual International Conference of the IEEE on Engineering in Medicine and Biology Society, Minneapolis, MN, USA, 2–6 September 2009; pp. 6107–6110.

30. Motoi, K.; Tanaka, S.; Kuwae, Y.; Yuji, T.; Higashi, Y.; Fujimoto, T.; Yamakoshi, K. Evaluation of a Wearable Sensor System Monitoring Posture Changes and Activities for Use in Rehabilitation. *J. Robot. Mechatron.* **2007**, *19*, 656–666.

31. Mannini, A.; Sabatini, A. On-line classification of human activity and estimation of walk-run speed from acceleration data using support vector machines. In Proceedings of the 2011 IEEE Annual International Conference of the IEEE Engineering in Medicine and Biology Society, Boston, MA, USA, 30 August–*3* September 2011; pp. 3302–3305.

32. James, D.A.; Davey, N.; Rice, T. An accelerometer based sensor platform for in situ elite athlete performance analysis. In Proceedings of the IEEE Sensors, Vienna, Austria, 24–27 October 2004; pp. 1373–1376.

33. Bächlin, M.; Förster, K.; Tröster. G. SwimMaster: A wearable assistant for swimmer. In Proceedings of the 11th International Conference on Ubiquitous Computing, Orlando, FL, USA, 30 September–3 October 2009; pp. 215–224.

34. Atallah, L.; Aziz, O.; Lo, B.; Yang, G.Z. Detecting walking gait impairment with an ear-worn sensor. In Proceedings of the 6th International Workshop on Wearable and Implantable Body Sensor Networks, Berkeley, CA, USA, 3–5 June 2009, pp. 177–182.

35. Farooq, M.; Sazonov, E. A Novel Wearable Device for Food Intake and Physical Activity Recognition. *Sensors* **2016**, *16*, 1067.

36. Fontana, J.M.; Farooq, M.; Sazonov, E. Automatic Ingestion Monitor: A Novel Wearable Device for Monitoring of Ingestive Behavior. *IEEE Trans. Biomed. Eng.* **2014**, *61*, 1772–1779.

37. Taniguchi, K.; Nishikawa, A.; Kawanishi, S.; Miyazaki, F. KOMEKAMI Switch: A Novel Wearable Input Device Using Movement of Temple. *Int. J. Robot. Mechatron.* **2008**, *20*, 260–272.

38. Amano, N.; Andoh, S.; Matsuoka, H.; Hashimoto, M.; Yamauchi, M.; Kubo, M.; Kawano, J. Changes in Chewing Rhythm During Repetitive Series of Mastication in Normal Adults as a Function of Time Elapsed and the Four Basic Taste Stimuli. *Nihon Hotetsu Shika Gakkai Zasshi* **1989**, *33*, 270–282. (In Japanese)

39. Liu, J.D.; Johns, E.; Atallah, L.; Pettitt, C.; Lo, B.; Frost, G.; Yang, G.Z. An Intelligent Food-Intake Monitoring System Using Wearable Sensors. In Proceedings of the 2012 9th International Conference on Wearable and Implantable Body Sensor Networks, London, UK, 9–12 May 2012; pp. 154–160.

40. Taniguchi K, Chiaki H, Kurosawa M, Nishikawa A. A novel earphone type sensor for measuring mealtime: consideration of the method to distinguish between running and meals. *Sensors*. 2017;17:252–266.

41. Inatomi S, Murata S, Hara H, Ihara T, Kamohara Y, Toyoda Y. Relationship between biting force and activities of daily living in the frail elderly. *Jpn J Health Prom*. 2013;15:37–41. (in Japanese)

42. Bite pressure measurement system T-scan III: http://www.nitta.co.jp/product/sensor/t-scaniii/ (in Japanese). Accessed September 11, 2017.

43. Occlusal force measuring system: http://www.gcdental.co.jp/ product/pdf/occluzer.pdf (in Japanese). Accessed September 11, 2017.

44. Watanabe K, Yamaguchi T, Gotouda A, Okada K, Mikami S, Hishikawa R. Analyses of unconstrained masseteric activity during the entire day by using an ultraminiature wearable electromyogram system. *J Jpn Soc Stomatog Fun*. 2014;19:125–136. (in Japanese)

45. Tanaka S, Uchikawa K, Maeda S, et al. An attempt to clear postoperative disorders through mastication visualization using wearable terminal. 72nd General Meeting of the Japanese Society of Gastroenterological Surgery, WS12-12; 2017 (in Japanese)

46. The occlusal force of an adult male during eating: https://www. jda.or.jp/park/relation/sport_06.html (in Japanese). Accessed September 11, 2017.

47. Kurosawa, M.; Taniguchi, K.; Nishikawa, A. A basic study of occlusal force measured using a wearable ear sensor. In Proceedings of the 14th International Conference on Ubiquitous Healthcare (uHealthcare 2017), Seoul, Korea, 5–7 December 2017.

48. Kurosawa, M.; Taniguchi, K.; Nishikawa, A. Earable: A novel earphone-type wearable sensor and its applications. In Proceedings of the 5th Annual

Conference of AnalytiX-2017, Session 7-4: Nanomaterial Applications in Chemical Sensors and Biosensors, Fukuoka, Japan, 22–24 March 2017; p. 400.

49. Taniguchi, K.; Kurosawa, M.; Nishikawa, A. Earable: Wearable ear computer. In Proceedings of the 2017 International Conference for Top and Emerging Computer Scientists (IC-TECS 2017), Taipei, China, 21–24 December 2017.

50. Nascimento, P.F.; Franco, A.P.G.O.; Fiorin, R.; Gomes, L.B.; Oliveira, V.; Abe, I.; Kalinowski, H.J. Characterization of the occlusal splints using optical fiber sensors. In Proceedings of the 2017 SBMO/IEEE MTT-S International Microwave and Optoelectronics Conference (IMOC), Águas de Lindóia, Brazil, 27–30 August 2017.

51. Jian, C.; Yi, Y.; Deng, L.; Luo, J. A device for multi-teeth bite force measurement. In Proceedings of the 2016 International Conference on Advanced Robotics and Mechatronics (ICARM), Macau, China, 18–20 August 2016.

52. Lin, K.R.; Liu, T.H.; Lin, S.W.; Chang, C.H.; Lin, C.H. Occlusive bite force measurement utilizing flexible force sensor array fabricated with low-cost multilayer ceramic capacitors (MLCC). In Proceedings of Transducers 2009–2009 International Solid-State Sensors, Actuators and Microsystems Conference, Denver, CO, USA, 21–25 June 2009.

53. Gonzalez, C.; Lantada, A. A wearable passive force sensor powered by an active interrogator intended for intra-splint use for the detection and recording of bruxism. In Proceedings of the 2009 3rd International Conference on Pervasive Computing Technologies for Healthcare, London, UK, 1–3 April 2009.

54. Kannan, A.; John, B.K.; Babu, D.S.; Kumar, M. Human biting force calculating instrument. In Proceedings of the 2017 International Conference on Circuit, Power and Computing Technologies (ICCPCT), Sasthancotta, India, 20–21 April 2017.

55. Tayel, M.; Elaskary, S.A.; Nassef, T.M. A bio-sensory system for increase implant longevity for occlusal analysis. In Proceedings of the 2012 2nd International Conference on Advances in Computational Tools for Engineering Applications (ACTEA), Beirut, Lebanon, 12–15 December 2012.

56. Kim, J.H.; McAuliffe, P.; O'Connel, B.; Diamond, D.; Lau, K.T. Development of bite guard for wireless monitoring of bruxism using pressure-sensitive polymer. In Proceedings of the 2010 International Conference on Body Sensor Networks, Singapore, 7–9 June 2010.

57. Nassef, T.M.; Tayel, M.B.; Elaskary, S.A. A proposed sensory setup to increase computational analysis accuracy for dental applications. In Proceedings of the 2013 International Conference on Computer Medical Applications (ICCMA), Sousse, Tunisia, 20–22 January 2013.

58. Waltimo, A.; Kononen, M. A novel bite force recorder and maximal isometric bite force values for healthy young adults. *Eur. J. Oral Sci.* **1993**, *101*, 171–175.

59. Fernandes, C.P.; Glantz, P.J.; Svensson, S.A.; Bergmark, A. A novel sensor for bite force determinations. *Dent. Mater.* **2003**, *19*, 118–126.

60. Braun, S.; Bantleon, H.S.; Hnat, W.P.; Freudenthaler, J.W.; Marcotte, M.R.; Johnson, B.E. A study of bite force, part 1: Relationship to various physical characteristics. *Angle Orthod.* **1995**, *65*, 367–372.

61. Braun, S.; Bantleon, H.P.; Hnat, W.P.; Freudenthaler, J.W.; Marcotte, M.R.; Johnson, B.E. A study of bite force, part 2: Relationship to various cephalometric measurements. *Angle Orthod.* **1995**, *65*, 373–377.

62. Palumbo, A.; Farella, M.; Avecone, S.; Pace, C.; Cocorullo, G. A system for simultaneous signals acquisition of EMG activity, bite force, and muscle pain, reveals the rotation of synergistic activity in the human jaw elevator muscles. In Proceedings of the 2007 IEEE Instrumentation & Measurement Technology Conference (IMTC 2007), Warsaw, Poland, 1–3 May 2007.

63. Goharian, N.; Moghimi, S.; Kalani, H. Estimation biting force based using EMG signals and Laguerre estimation technique. In Proceedings of the 2015 23rd Iranian Conference on Electrical Engineering, Tehran, Iran, 10–14 May 2015.

64. Poomsombut, S.; Limsakul, C.; Phukpattaranont, P. Appropriate features to determine correlation in EMG signals and biting force in occlusion system. In Proceedings of the 2018 International Conference on Embedded Systems and Intelligent Technology & International Conference on Information and Communication Technology for Embedded Systems (ICESIT-ICICTES), Khon Kaen, Thailand, 7–9 May 2018.

65. Yu, H.; Sun, Y.; Bai, F.; Ren, H. A preliminary study of force estimation based on surface EMG: Towards neuromechanically guided soft oral rehabilitation robot. In Proceedings of the 2015 IEEE International Conference on Rehabilitation Robotics (ICORR), Singapore, 11–14 August 2015.

66. Ferrario, V.F.; Sforza, C.; Zanotti, G.; Tartagilia, G.M. Maximal bite force in healthy young adults as predicted by surface electromyography. *J. Dent.* **2004**, *32*, 451–457.

67. Van Der Bilt, A.; Tekamp, F.A.; Van Der Glas, H.W.; Abbink, J.H. Bite force and electromyography during maximum unilateral and bilateral clenching. *Eur. J. Oral Sci.* **2008**, *116*, 217–222.

68. Taniguchi, K.; Kurosawa, M.; Kimura, Y.; Nishikawa, A. A basic study for estimation of occlusal force using an ear wearable sensor. *Electron. Commun. Jpn.* **2018**, *101*, 20–27.

69. Fastier-Wooller, J.; Phan, H.P.; Dinh, T.; Nguyen, T.K.; Cameron, A.; Öchsner, A.; Dao, D.V. Novel low-cost sensor for human bite force measurement. *Sensors* **2016**, *16*, 1244

Chapter 7:
Accomplishments

7.1 Publications in Journal

1. Taniguchi K, Chiaki H, Kurosawa M, Nishikawa A. A novel earphone type sensor for measuring mealtime: Consideration of the method to distinguish between running and meals. *Sensors* **2017**, *17* (2), p. 252 (14 pages).

2. Taniguchi K, Kondo H, Kurosawa M, Nishikawa A. Earable TEMPO: A novel, hands-free input device that uses the movement of the tongue measured with a wearable ear sensor. *Sensors* **2018**, *18* (3), p. 733 (11 pages).

3. Taniguchi K, Kurosawa M, Kimura Y, Nishikawa A, A basic study for estimation of occlusal force using an ear wearable sensor. *IEEJ Transactions on Electronics, Information and Systems* **2018**, *138* (6), pp. 648-654 (in Japanese).
   English Translation: *Electronics and Communications in Japan* **2018**, *101* (11), pp. 20-27.

4. Kurosawa M, Taniguchi K, Momose H, Sakaguchi M, Kamijo M. Nishikawa A. Simultaneous Measurement of Ear Canal Movement, Electromyography of the Masseter Muscle and Occlusal Force for Earphone-Type Occlusal Force Estimation Device Development. *Sensors* **2019**, *19* (15), p. 3441 (16 pages).

6.2 Conferences

[International]

1. ●Kurosawa M, Nishikawa A. The Control of Human Fingers by Using Functional Electrical Stimulation. The 7th International Symposyum on High-Tech Fiber Engineering for Young Researcher, Suzhou, China, November 2015. <Oral and Poster>

2. ●Kurosawa M, Nishikawa A. Analyzing Surface Electromyogram from Flexor Digitorum Superficialis and Extensor Digitorum Communis. The 38th Annual International Conference of the IEEE Engineering in Medicine and Biology Society (EMBC'16), Florida, USA, August 2016. <Poster> [Peer-reviewed]

3. ●Kurosawa M, Taniguchi K, Nishikawa A. Earable: A novel earphone-type wearable sensor and its applications. The 5th Annual Conference of AnalytiX-2017, Fukuoka, Japan, March 2017. <Oral> [Invited]

4. Takemura K, Kurosawa M, ●Atsuumi K, Matsui K, Miyazaki F, Nishikawa A. Frequency Domain System Identification of Human Finger Dynamics Using Functional Electrical Stimulation based on an Agonist-Antagonist Concept. REHABWEEK 2017/ 2017 Annual Conference of the International Functional Electrical Stimulation Society (IFESS 2017), London, UK, July 2017. <Poster> [Peer-reviewed]

5. ●Kurosawa M, Taniguchi K, Nishikawa A. A basic study of occlusal force measured using a wearable ear sensor. The 14th International Conference on Ubiquitous Healthcare (uHealthcare 2017), Seoul, Korea, December 2017. <Poster> [Peer-reviewed]

6. Taniguchi K, ●Kurosawa M, Nishikawa A. Earable: Wearable ear computer. In Proceedings of the 2017 International Conference for Top and Emerging Computer Scientists (IC-TECS 2017), Taipei, China, December 2017. <Oral> [Invited]

7. ●Kurosawa M, Taniguchi K, Nishikawa A. Earable: A novel earphone-type wearable sensor and its applications. Textile Summit 2018, Nagano, Japan 2018. <Poster>

[Domestic (in Japanese)]

1. 黒澤真美, 西川敦. 機能的電気刺激を用いた手指機能の再現制御. 第 4 回信州ロボット研究会. ポスター・支部会（2014 年 11 月発表）

2. 黒澤真美, 西川敦. 機能的電気刺激（FES）を用いた手指機能の再現制御 －浅指屈筋・総指伸筋を対象とした表面筋電図の計測－. 第 5 回信州ロボット研究会. ポスター・支部会（2015 年 11 月発表） ＊特別賞＊

3. 黒澤真美, 谷口和弘, 西川敦. 耳装着型デバイス“earable”を用いた噛み締め

動作の検出と外部機器操作用スイッチ動作としての利用可能性の基礎検討. 生体医工学シンポジウム 2017. ポスター・本大会（2017 年 9 月発表）

4. 黒澤真美, 谷口和弘, 西川敦. 耳装着型センサ earable を用いた咬合力計測のための基礎検討, 信州ロボット研究会. ポスター・支部会（2018 年 3 月発表）

5. 黒澤真美，谷口和弘，百瀬英哉，坂口正雄，上條正義，西川敦. イヤホン型咬合力推定装置開発のための外耳道の動きと咬筋電位ならびに咬合力の同時計測とその分析. 第 58 回日本生体医工学会大会. ポスター・本大会（2019 年 6 月発表）

Chapter 8:

Acknowledgement

This work was supported by a Grant-in-Aid for the Shinshu University Advanced Leading Graduate Program by the Ministry of Education, Culture, Sports, Science and Technology (MEXT), Japan. This study was partly supported by the Regional ICT-Promoting Research and Development Program (132308004) of the Strategic Information and Communications R&D Promotion Programme (SCOPE) by the Japanese Ministry of Internal Affairs and Communications, and Innovation Program, Wearable Earring Computer by the Ministry of Internal Affairs and Communications, and JSPS KAKENHI Grant Number JP19K12828.

I would like to express my deepest gratitude to all the subjects who were involved in these experiments.

Firstly, I would like to express my sincere gratitude to my supervisor Prof. Atsushi Nishikawa in Osaka University for the continuous support of my study since the days of an undergraduate student in Shinshu University, for his patience, motivation, and immense knowledge. His long-term guidance helped me in all the time of research at the both environment of Shinshu University and Osaka University. Without his encouragement, this thesis would not have been possible. I could not have imagined having a better advisor and mentor for my study.

My deepest appreciation goes to Prof. Masayoshi Kamijo, Prof. Hiroaki Yoshida, Prof. Hiroaki Ishizawa and Prof. Michihiko Koseki in Shinshu University, and Dr. Takeshi Fujita in Kobe University for their significant contribution and extensive discussion as a member of the Board of Examiners for my thesis.

I also would like to express my gratitude to Dr. Kazuhiro Taniguchi in Hiroshima City University, for the great collaborative research about earable. I could have studied these theme thanks of his support and advice. Prof. Emerit. Masao Sakaguchi in National Institute of Technology Nagano College and Mr. Hideya

Momose in SKINOS NAGANO Co., Ltd. have made enormous contribution to preparing necessary equipment for my research. Mr. Keita Atsuumi in Hiroshima City University, Dr. Kazuhiro Matsui in Osaka University and all team meeting member have given me constructive comments and warm encouragements.

Then I appreciate Prof. Hiroaki Yoshida and Prof. Satoshi Hosoya for warmly accepting my laboratory rotation for a month, and keeping support me with their helpful advice to study biometric measurement. Prof. Masayoshi Kamijo also have accepted my request to keep my name on his laboratory, and supported me with insightful comments. They also have willingly approved me to use equipment in their laboratory in Shinshu University.

About a period I had studied in Sweden, I would like to express deep appreciation to Dr. Joel Peterson in University of Borås for giving me many opportunities to study wearable technologies and to experience in Sweden. His tremendous support has given me many inspirations not only about research but also about my future plans, with my host mother and friends in Sweden.

Prof. Emerit. Mikihiko Miura, Prof. Shigeru Inui, Prof. Emerit. Hajime Konishi, Prof. Tsutomu Ishiwatari have gave moral support and encouragement to me as a mentor in Shinshu University. Without them, I could have never continued trying in the both Leading Program and general university life. All the Leading Program staff's support were also invaluable.

Other thanks go to all of my lab mates through seven years in Shinshu University and Osaka University for the stimulating discussion, giving inspirations and helping to take a balance between work and rest.

Lastly, I would like to express the deepest appreciation to my family and my partner for supporting me mentally, financially and motivationally thorough out my long student time and my life in general.